MICHIGAN STATE UNIVERSITY LIBRARIES

3 1293 01417 2583

This is to certify that the

dissertation entitled

RELATION BETWEEN PHOSPHATE SORPTION AND AGGREGATION

IN OXISOLS FROM BRAZIL

presented by

Jose Maria de Lima

has been accepted towards fulfillment
of the requirements for

_____PhD_____ degree in _Crop and Soil_ Sciences

Sharon J Anderson
Major professor

Date 7/25/95

PLACE IN RETURN BOX to remove this checkout from your record.
TO AVOID FINES return on or before date due.

DATE DUE	DATE DUE	DATE DUE
_____	_____	_____
_____	_____	_____
_____	_____	_____
_____	_____	_____
_____	_____	_____
_____	_____	_____
_____	_____	_____

MSU Is An Affirmative Action/Equal Opportunity Institution

c:\circ\datedue.pm3-p.1

RELATION BETWEEN PHOSPHATE SORPTION AND AGGREGATION IN OXISOLS FROM BRAZIL

By

Jose Maria de Lima

A DISSERTATION

Submitted to
Michigan State University
in partial fulfillment of the requirements
for the degree of

DOCTOR OF PHILOSOPHY

Department of Crop and Soil Sciences

1995

ABSTRACT

RELATION BETWEEN PHOSPHATE SORPTION AND AGGREGATION IN OXISOLS FROM BRAZIL

By

Jose Maria de Lima

Phosphate sorption and the stability and size of aggregates are strongly related to type and concentration of iron oxides in Oxisols. The main features of Oxisols are their stable and small aggregates, especially in the B horizon of those soils with medium to high iron oxide content. Aggregation affects some chemical reactions in soils, physically by decreasing the exposure of particle surfaces to solution, and chemically through differences in composition within the different aggregate sizes. The physical effect occurs mostly in short time reactions, where time is insufficient for solution to reach sites in particle interiors. Phosphate sorbed in inner-sphere complexes brings negative charge to the surface of particles, which increases particle repulsion. Eventually, P sorption disrupts the aggregates, increasing the amount of clay-sized particles in suspension. The objectives of this research were to evaluate whether aggregate composition varies with size; to measure the effect of aggregation and aggregate size on the amount of dithionite- and oxalate-extractable Fe and Al; to measure the effect of phosphate sorption on isoelectric point and clay dispersion ; and to measure the effect of aggregation and of aggregate size and composition on phosphate sorption kinetics in 1- to 2-mm and 0.125- to 0.25-mm aggregates of A and B horizons from two Oxisols with 165 g kg^{-1} Fe$_2$O$_3$ but different hematite:goethite ratios. Disaggregation of aggregates increased the amount of dithionite- and oxalate-extractable Fe and Al. Phosphate sorption decreased electrophoretic mobility and

isoelectric point of B horizon aggregates, especially in the higher hematite:goethite soil. As P sorption decreased the isoelectric point (IEP) to values near the suspension pH and net positive charge decreased, the amount of dispersed clay decreased. Then, as IEP values became lower than suspension pH, P sorption increased the amount of clay dispersion. Small aggregates had less dispersed clay/total clay than large aggregates. Disaggregation of aggregates increased P sorption rates at short times (8 min), especially in the B horizon samples. There was no effect of aggregate size on P sorption kinetics. Aggregates from B horizon had higher initial sorption rate than those from A horizon.

To Annete, Drielle, Elisa, and Alexandre,

for their love and support.

To my parents Antonio and Clarice,

for the opportunity of life.

ACKNOWLEDGMENTS

Table of Contents

Chapter 1

Chapter 2

Chapter 3

Chapter 4

List of Tables

List of Figures

x

Chapter 1

General Introduction

Aggregation and phosphate sorption in Oxisols (Latosols) are strongly affected by type and crystallinity of iron oxides (Bigham, et al., 1978; Curi and Franzmeier, 1984). Differences among classes of Oxisols are also mostly dependent on type and content of iron oxides (Resende et al., 1988; Oliveira et al., 1992). Some Oxisols, even those having similar amounts of iron oxides, can be different in color due the proportion of hematite and goethite in the clay fraction. These Oxisols can have different responses to phosphate sorption, and such differences can be related to aggregation and aggregate size, besides the type of iron oxides.

Higher moisture content during soil formation favors goethite instead of hematite (Curi and Franzmeier, 1984; Macedo and Bryant, 1987; Schwertmann and Taylor, 1989; Schwertmann, 1993). Climate, topographic position, and drainage play important roles in regulating soil moisture and the relative proportions of hematite and goethite. In soils derived from metamorphic rocks (e.g., mica schists) the orientation of the strata can control soil drainage. In areas where faulting has occurred, a soil developed in vertical or inclined schists may be better drained (and have higher hematite:goethite ratio and lower $SiO_2:Al_2O_3$) than an adjacent soil developed in horizontal schists (Richardson and Daniels, 1993; Chagas, 1994).

Aggregate stability and aggregate composition can differ between soil horizons, or even within the same horizon, among different aggregate sizes, due to differences in organic matter and iron oxides. Crystalline iron oxides (i.e.,

hematite and goethite) tend to form microaggregates among themselves
(Schwertmann and Kämpf, 1985). Other researches have indicated that
macroaggregates are formed of microaggregates and of individual particles, with
organic matter and some amorphous oxides as cementing substances (Giovanini
and Sequi, 1976; Tisdall and Oades, 1982; Barberis et al., 1991). Therefore, A
horizons, with their higher organic matter and amorphous oxide contents, are
more likely to have larger aggregates than B horizons.

Aggregation is a physical parameter closely related to charge. In Oxisols,
because most of the surface charge is pH-dependent, aggregation is also pH-
dependent. In pH-dependent soils, such as Oxisols, the isoelectric point (IEP)
represents the pH at which net surface charge vanishes (Figure 1.1). Thus, if the
soil pH coincides with the IEP, the soil has the same amount of positive and
negative charge, the *net* surface charge is zero. The soil will have *net* negative
charge if the pH is higher than the isoelectric point and *net* positive charge if the
pH is below the isoelectric point (Figure 1.1). Iron and aluminum oxides have
isoelectric points near pH 8-9, whereas kaolinite and organic matter have lower
IEP values. Therefore, Oxisols, which typically have pH between 4 and 6, often
bear a small *net* positive charge, especially in B horizons. In A horizons, organic
matter can import a low *net* negative charge. Because net charge of Oxisols is
near zero at natural soil pH, the number of positively charged sites is nearly equal
to the number of negatively charged sites, so particle-particle interactions are
attractive rather than repulsive. This strong particle-particle attraction is
responsible for the high aggregate stability in Oxisols.

Sorption of anions in inner-sphere[1] complexes decreases positive charge
and increases negative charge in soils. Phosphate sorption is one of the most

---

[1] Complexes where the ion reacts directly with the surface of the mineral or organic matter, with no water
molecules interposed between the ion and the surface (Sposito, 1989 p.68).
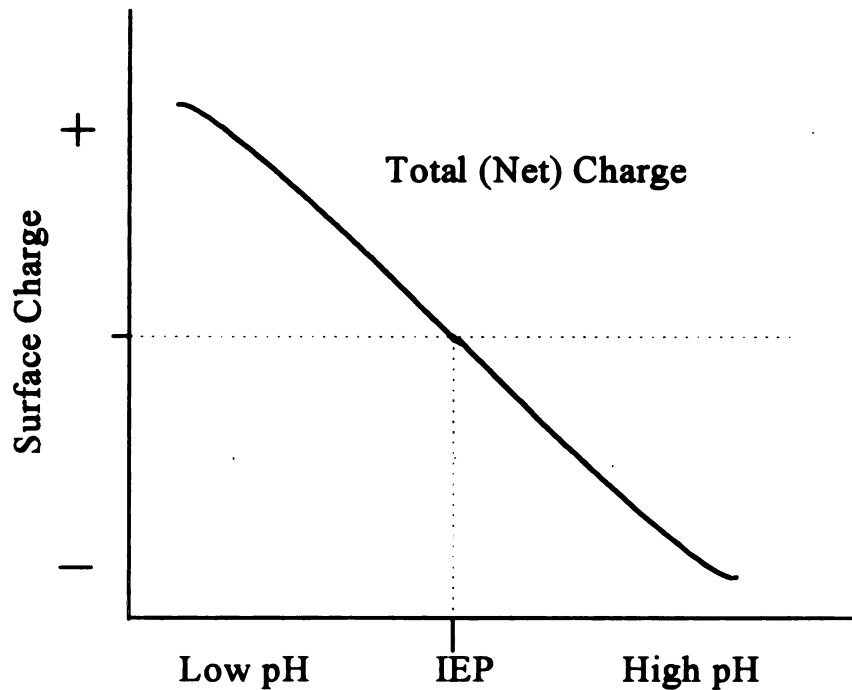
Figure 1.1. Schematic representation of the effect of pH on surface charge.

important inner-sphere complexes in Oxisols. The high amount of oxides is responsible for high quantities of phosphate sorbed in these soils. Changes in the charge balance by phosphate sorption can also be a problem in soil physics, since it can decrease aggregate stability, increasing the quantity of particles and microaggregates in suspension, resulting in higher soil erosion. Inner-sphere sorption of phosphate on the hydroxylated mineral surfaces releases OH (or H_2O) in a process called ligand exchange (Figure 1.2).
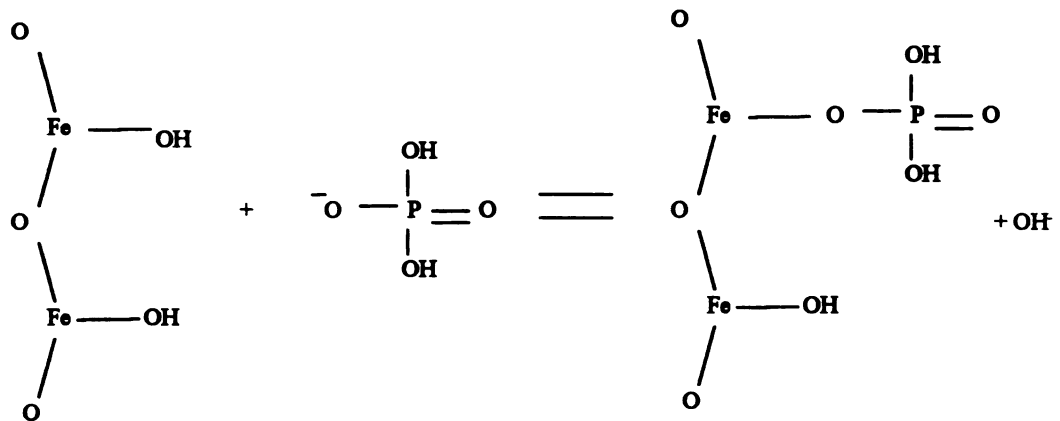
Figure 1.2. Schematic representation of ligand exchange mechanism for phosphate adsorption on the surface of iron oxide.

Complexes formed between phosphate ions and Fe oxides can be monodentate or bidentate (Figure 1.3). The bidentate complexes are more stable than the monodentate, which causes sorption to be mostly "irreversible".

Monodentate Complex   Bidentate Complex
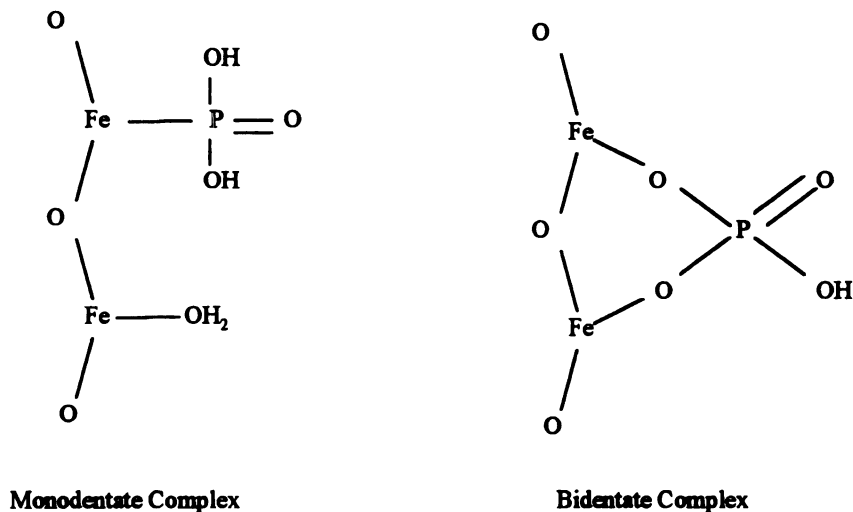
Figure 1.3. Schematic representation of the possible complexes formed during phosphate sorption on the surface of iron oxide.

Phosphate that is sorbed in inner-sphere complexes is difficult to desorb, especially when P is sorbed by bidentate complex (Kafkafi, 1967); thus, adsorption kinetics is much faster than desorption kinetics. Much of the phosphate fertilizer added to Oxisols is "irreversibly" sorbed in inner-sphere complexes and is not readily available to plants. Phosphate sorption kinetics in Oxisols must be known in order to maximize the efficiency of P fertilization and to minimize the potentially adverse effects of P sorption on soil physical properties. Phosphate sorption kinetics can be affected by both aggregation and aggregate size. Reactive sites in the interior of aggregates are not in direct contact with bulk soil solution, so sorption of solution-phase phosphate by interior sites will depend on transport (i.e., diffusion) of the phosphate to the sorption site, not just on the chemical kinetics of the sorption reaction. Thus, reaction rates measured in the laboratory on disaggregated samples are not indicative of sorption rates in the field, where Oxisols generally are strongly aggregated. In addition to the effect of aggregation *per se* on sorption kinetics, the size of aggregates may also affect sorption kinetics. In the simplest scenario, phosphate sorption should be faster on small aggregates, which have a smaller radius and, by inference, shorter diffusion path. However, the effect of aggregate size on P sorption kinetics is much more difficult to predict if tortuosity differs between large and small aggregates, for example if tortuosity depends on the openness of the aggregate structure or on the type and crystallinity of iron oxides.

This research relates phosphate sorption and sorption kinetics to aggregation and to aggregate size and composition in two Oxisols (Latosols in FAO classification). Two aggregate size fractions from A and B horizons of a Yellow-Red Latosol and a Dark-Red Latosol from southeast Brazil (Figure 1.4) were used. Both soils contain about 165 g kg^{-1} Fe$_2$O$_3$ (Table 1.1), but the Dark-Red Latosol formed on a mica schist in which the strata were steeply inclined (Figure 1.4). Thus the Dark-Red Latosol is well drained and has relatively high
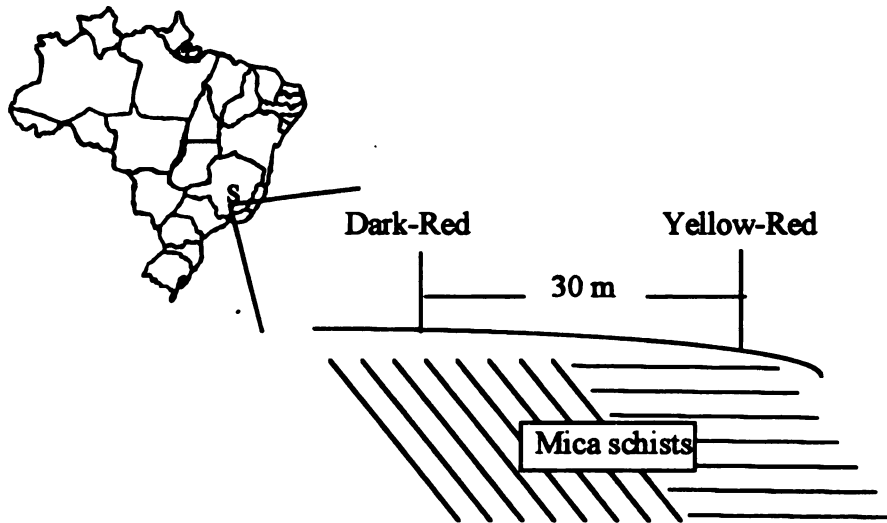
Figure 1.4. Sampling region (S) in Brazil and diagram of the soil parent material.

Table 1.1. Chemical composition[1] and color[2] of A and B horizons of two Oxisols from Brazil.

Horiz	SiO$_2$	Al$_2$O$_3$	Fe$_2$O$_3$	TiO$_2$	P$_2$O$_5$	Mn	Color
			g kg^{-1}				
			Yellow-Red Latosol				
A	159	299	162	12.3	0.2	217	5YR 4/4
B	153	304	170	12.3	0.1	152	4YR 5/6
			Dark-Red Latosol				
A	125	318	165	11 .0	0.2	111	2.5YR 3/5
B	82	341	169	11.6	0.1	110	2.5 YR 4/8

1 - Measured in the H$_2$SO$_4$ (1:1 acid:water) extract: SiO$_2$ was measured by gravimetry, after dissolving the residue with sodium carbonate solution and reprecipitating with H$_2$SO$_4$; Al$_2$O$_3$ was measured by coplexometry with EDTA; Fe$_2$O$_3$ and Mn were measured by atomic absorption; P$_2$O$_5$ and TiO$_2$ were measured by colorimetry (Vettori, 1969; EMBRAPA, 1979).

2 - Measured in the moisten sample by comparison with the Munsell Color Chart for soils.

hematite:goethite ratio, which gives it dark red color, and a high gibbsite:kaolinite ratio (Table 1.2). The Yellow-Red Latosol, which was collected just 30 m away from the Dark-Red Latosol, formed on nearly horizontal strata, and thus is more poorly drained. Therefore, the YR soil has relatively less hematite (more goethite) and a correspondingly yellow color, in spite of its fairly high Fe oxide content (Table 1.2). Both soils also contain small amounts of illite (mica) and hydroxy-interlayer vermiculite (Chagas, 1994). Some physical, chemical, and mineralogical properties of these soils are shown in Tables 1.1 and 1.2. Because of differences in hematite:goethite and gibbsite:kaolinite ratios, the two soils may differ in aggregate stability and their reactivity toward phosphate sorption.

The objectives of this research were:

a) To measure the effect of aggregation and aggregate size on dithionite-citrate-bicarbonate (DCB) and ammonium-oxalate extractable Fe and Al, and to determine whether different aggregate sizes differ in composition (Chapter 2);

b) to determine the effect of phosphate sorption and aggregate size on isoelectric point and dispersion of clay (Chapter 3).

c) to determine the effect of aggregation and aggregate size and composition on phosphate sorption kinetics (Chapter 4).

Table 1.2. Physical, chemical, and mineralogical properties of A and B horizons of two Oxisols from Brazil .

Horiz	Clay[1]	Carb[2]	Fe_o[3]	Al_o[3]	Fe_d[4]	Al_d[4]	Fe_o/Fe_d	Hm[5]	Gt[5]	Hm/Gt	Gb[6]	Kt[6]	Gb/Kt
			g (kg soil)$^{-1}$					g (kg soil)$^{-1}$			g (kg soil)$^{-1}$		
					Yellow-Red Latosol								
A	711	15.8	1.20	1.79	101	29	0.012	14	143	0.10	267	343	0.78
B	721	9.2	0.59	1.63	114	30	0.005	19	158	0.12	286	347	0.82
					Dark-Red Latosol								
A	691	18.8	1.88	2.04	99	31	0.019	25	126	0.20	350	240	1.46
B	753	11.0	0.65	1.79	114	32	0.006	34	141	0.24	383	263	1.46

1 - Clay content was measured by the pipette method, dispersing with NaOH (USDA, 1992).
2 - Total carbon was measured by high-temperature combustion.
3 - Oxalate-extractable Fe and Al measured with ammonium oxalate, using 1:40 soil:solution ratio, 2h shaking time, and one extraction (Schwertmann, 1964).
4 - Dithionite-citrate-bicarbonate extracted Fe and Al, measured according to Mehra and Jackson (1958), using 1:40 soil: solution ratio in 4 successive extraction.
5 - Amount of hematite and goethite in the clay fraction, measured using the ratio of intensities of the peaks 012 of Hm and 110 of Gt (Kämpf and Schwertmann, 1982).
6 - Kaolinite and gibbsite were measured by differential thermal analysis, using endothermic peaks at 550 and 350° C, respectively.

Bibliography

Barberis, E., F.A. Marsan, V. Boero, and E. Arduino. 1991. Aggregation of soil particles by iron oxides in various size fractions of soil horizons. J. Soil Sci. 42:535-542.

Bigham, J.M., D.C. Golden, S.W. Buol, S.B. Weed, and L.H. Bowen. 1978. Iron oxide mineralogy of well-drained Ultisols and Oxisols: II. Influence on color, surface area, and phosphate retention. Soil Sci. Soc. Am. J. 42:825-830.

Chagas, C.S. 1994. Associação de Latossolo Variação Una e Latossolo Vermelho-Escuro: efeito diferencial da orientação dos estratos de rochas pelíticas pobres. Lavras, MG - Brazil. Escola Superior de Agricultura de Lavras. 124p. (M.S. Theses)

Curi, N., and D.P. Franzmeier. 1984. Toposequence of Oxisols from the Central Plateau of Brazil. Soil Sci. Soc. Am. J. 48:341-346.

Empresa Brasileira de Pesquisa Agropecuaria. Serviço Nacional de Levantamento e Conservação de Solos. 1979. Manual de métodos de análises de solo. Rio de Janeiro, 1979. 247p.

Giovannini, G., and P. Sequi. 1976. Iron and aluminum as cementing substances of soil aggregates. II. Changes in stability of soil aggregates following extraction of iron and aluminum by acetylacetone in a non-polar solvent. J. Soil Sci. 27:148-153.

Kafkafi, U., A.M. Posner, and J.P. Quirk. 1967. Desorption of phosphate from kaolinite. Soil Sci. Soc. Amer. Proc. 31:348-353.

Kämpf, N., and U. Schwertmann. 1982. Quantitative determination of goethite and hematite in kaolinitic soils by x-ray diffraction. Clay Miner. 17:359-363.

Macedo, J., and R.B. Bryant. 1987. Morphology and genesis of a hydrosequence of oxisols in Brazil. Soil Sci. Soc. Am. J. 51:690-698.

Mehra, O.P., and M.L. Jackson. 1958. Iron oxide removal from soils and clays by a dithionite-citrate system buffered with sodium bicarbonate. Clays and Clay Miner. 7:317-327.

Oliveira, J.B., P.K.T. Jacomine, and M.N. Camargo. 1992. Classes gerais de solos do Brasil: guia auxiliar para seu reconhecimento. Jaboticabal, FUNEP. 201p.

Resende, M., N. Curi, and D.P. Santana. 1988. Pedologia e fertilidade do solo: interações e aplicações. Lavras: ESAL, Piracicaba:POTAFOS. 81p.

Richardson, J.L., and R.B. Daniels. 1993. Stratigraphic and hydraulic influences on soil color development. p. 109-125. In: J.M. Bigham and E.J. Ciolkosz, (ed.) Soil color. SSSA Spec. Publ. 31. SSSA, Madison, WI.

Schwertmann, U. 1964. Differenzierung der eisenoxide des bondes durch extraktion mit ammonium-oxalat-losung. Zeitschrift fuer Pflanzenernahrung. 105:194-202.

Schwertmann, U. 1993. Relations between iron oxides, soil color, and soil formation. p. 51-69. In: J.M. Bigham and E.J. Ciolkosz, (ed.) Soil color. SSSA Spec. Publ. 31. SSSA, Madison, WI.

Schwertmann, U., and N. Kämpf. 1985. Properties of goethite and hematite in kaolinitic soils of Southern and Central Brazil. Soil Sci. 139:344-350.

Schwertmann, U., and R.M. Taylor. 1989. Iron oxides. p.379-438. In: J.B. Dixon, and S.B. Weed, (ed.) Minerals in soil environments. 2nd ed. SSSA Book Ser. 1. SSSA, Madison, WI.

Sposito, G. 1989. The chemistry of soils. New York, Oxford University Press. 277p.

Tisdall, J.M., and J.M. Oades. 1982. Organic matter and water-stable aggregates in soils. J. Soil Sci. 33:141-163.

United States Department of Agriculture, Soil Survey Laboratory Staff. 1992. Soil survey laboratory method manual. Soil Survey Investigation Report No. 42. 400p.

Vettori, L. 1969. Métodos de análises de solos. Rio de Janeiro, Ministerio da Agricultura, 24p. (Boletim Técnico, 7).

Chapter 2

Aggregation and Aggregate Size Effect on Selected Properties of Two Oxisols From Brazil

Abstract

Aggregation and aggregate size can affect the results of chemical and physical analyses in the < 2-mm size fraction of soils, especially in Oxisols with high amounts of Fe and Al oxides, which have high aggregate stability and small aggregates. This research verifies whether 1- to 2-mm and 0.1- to 0.2-mm aggregates of A and B horizon of two Oxisols differ in clay, carbon, and Fe and Al oxide contents, and measures how aggregation and aggregate size regulates dithionite-citrate-bicarbonate (DCB) and oxalate extractability of Fe and Al oxides in these soils. In the A horizon, small aggregates had lower amounts of clay and of Fe and Al extracted by DCB and oxalate than did large aggregates, but aggregate size had no effect on these measurements in the B horizon. The amount of goethite was smaller in small aggregates of both A and B horizons. This caused the ratio hematite/goethite to be smaller in large aggregates. Disaggregation increased the amount of DCB- and oxalate extractable Fe and Al, even after four successive extractions, except for small aggregates in A horizon. Thus, aggregates must be destroyed in order to quantify the true amount of Fe and Al oxides in these Oxisols.

Introduction

Strong aggregation is one of the most common physical features of Oxisols, particularly those with medium to high content of iron oxides. The mineralogy of these soils is dominated by the presence of kaolinite, hematite, goethite, and gibbsite (Resende, 1976; Fontes, 1992). Even though there are controversies about the role of oxides in soil aggregation, it is known that the crystalline part of DCB-extractable (free) Fe oxides in Oxisols form microaggregates among themselves (Schwertmann and Kämpf, 1985), though they also form aggregates by interacting with other clay minerals and gibbsite (Fontes, 1992). Barberis et al. (1991) showed that when soils had hematite/(hematite+goethite) (i.e., $Hm/Hm+Gt$) > 0.3, aggregates were more resistant to DCB and oxalate extraction than if the soils had a lower $Hm/(Hm+Gt)$ ratio (i.e., more goethite). These results suggest either that hematite promotes aggregate stability more than does goethite, or that hematite, which has a lower surface area than goethite, is more difficult to dissolve than goethite. Because hematite and goethite form microaggregates by interacting among themselves (Schwertmann and Kämpf, 1985), hematite and goethite concentrations may both be greater in microaggregates than in large aggregates.

Organic matter can combine microaggregates together into macroaggregates larger than 0.25 mm in many types of soils (Giovanini and Sequi, 1976; Tisdall and Oades, 1982). In Oxisols, large and medium sized aggregates may be a combination of clay particles, organic matter and microaggregates of Fe minerals (Santos, 1989). Thus, larger aggregates should have higher organic carbon concentration than smaller aggregates.

Although amorphous iron oxides are present in small amounts in Oxisols, they are very effective in aggregating soil particles (Arduino et al., 1989; Barberis et al., 1991). Organic matter inhibits crystallization of Fe and Al oxides, so amorphous oxide concentrations are positively correlated with organic matter.

Thus, amorphous oxide concentrations are generally higher in A than B horizons. Further, if organic C is higher in large than small aggregates, then amorphous Fe and Al oxides (i.e., oxalate-extractable) may be greater in large than small aggregates.

Aggregation and aggregate size can affect the results of chemical extraction in the < 2-mm size fraction used for most chemical and physical analyses. Moura Filho and Buol (1976) found that the extractable concentrations of exchangeable cations and phosphate increased as aggregate size decreased in three < 2-mm aggregate size fractions, and that disaggregation of aggregates increased the extractable concentrations of exchangeable cations and phosphate. Other chemical extractions may also be affected by aggregation and possibly by aggregate size in this range of aggregate size in Oxisols.

The objectives of this study were to test the hypotheses that aggregation limits the extractability of Fe and Al from Oxisols, and that aggregation will more severely limit Fe and Al extraction from large than small aggregates. An additional goal was to determine whether organic matter concentrations are higher in large aggregates and whether crystalline Fe oxides, particularly hematite, are more abundant in small than large aggregates because of tendency for hematite particles to form microaggregates by associating with one another rather than with kaolinite or gibbsite.

Materials and Methods

Aggregate Fractionation

Samples were collected from A and B horizons of two Oxisols that have similar amounts of total iron oxides (165 g kg^{-1}) but differ in hematite:goethite and gibbsite:kaolinite ratios. The two soils, a Yellow-Red Latosol (Una Variant),

hereafter referred to as YR, and a Dark-Red Latosol (hereafter DR) were collected about 30 m apart from one another in the "Campos das Vertentes" Region, Minas Gerais State, Brazil. Some physical, chemical, mineralogical, and morphological properties of the bulk sample of each horizon are reported elsewhere (Tables 1.1 and 1.2, Chapter 1). The soil samples were air-dried, each whole sample was placed in the top sieve in a nest of sieves with 2-mm, 1-mm, 0.25-mm and 0.125-mm sieves to separate 1- to 2-mm and 0.125- to 0.25-mm aggregates. Then, the 1- to 2-mm and 0.125- to 0.25- mm aggregates were placed on the top of 1-mm sieve and 0.125 mm sieve, respectively, and the nest of sieves connected to a motor that moved 3 cm up and down (35 cycles per min) in a solution of 0.01 M $CaCl_2$ for 15 min. The $CaCl_2$ solution then was replaced with deionized water, and the sieve nest was raised and lowered for 15 min in deionized water. The equipment used to wet-sieve the samples is the same used for measuring aggregate stability described in Yoder (1936). The water-stable aggregates in each size fraction were dried for 24 h at 40 °C in a ventilated oven. A total of eight dried aggregate samples (two aggregate sizes from two horizons of each of two soils) were used in the experiments described below.

Particle-size Distribution

Particle size distribution was measured in triplicate by the pipette method (USDA, 1992) using 20 g of aggregates that first were physically dispersed by shaking for 15 min in 500 ml of 2 mM NaOH in a blender at 12,000 rpm. The suspensions were transferred to a graduated cylinder, and the final volume of suspension brought to 1000 ml with deionized water. After 7.5 h, a 25-ml aliquot was withdrawn from 10-cm depth in the suspension, placed in a weighed aluminum dish and dried to quantify the amount of clay (g kg^{-1}) in the aggregates. Sand was measured in the fraction that was retained in the 0.05-mm sieve, and the content of silt was calculated by the difference between the whole 20 g of aggregates and the masses of clay and sand.

Iron and Aluminum Extractions

The concentrations of Fe and Al extractable by acid ammonium oxalate (hereafter referred to as oxalate) and by dithionite-citrate-bicarbonate (DCB) were measured in triplicate on aggregated and disaggregated samples. For each aggregate size, 1 g of aggregates was placed in each of six 50-ml centrifuge tubes and prewetted with a few drops of deionized water. After about 30 min, 10 ml of deionized water was added to each tube. Half of the samples were disaggregated by sonicating for 2 min at 100 Watts. Clay was released (dispersed) during sonication but flocculated almost immediately after the sonicator was turned off. Therefore, the sonicated samples used in these extractions are not truly dispersed and are referred to as disaggregated.

Oxalate-extractable Fe and Al were extracted by adding 30 ml of 0.26 M $(NH_4)_2C_2O_4$, adjusted to pH 3 with 0.2 M $H_2C_2O_4$, to the 1 g of aggregated or disaggregated samples and 10 ml of deionized water in each tube. The final oxalate concentration was 0.2 M (Schwertmann, 1964). The tubes were shaken in the dark for 2 h at 20 ± 2 °C and then centrifuged, also in the dark, for 5 min at 1500 rpm. The supernatant solutions were decanted and saved for Fe and Al measurements by atomic absorption, in an air-acetylene and N_2O-acetylene flames, respectively. Standards for atomic absorption were prepared in 0.2 M ammonium oxalate solution. Extractable Fe and Al concentrations were calculated as:

$$Fe \ or \ Al \ (\text{g kg}^{-1} \text{ aggregate}) = C \ \text{x} \ V / M_{aggr} \qquad (2.1)$$

where C is the Fe or Al concentrations in the supernatant solution, V is the total solution volume, and M_{aggr} is aggregate mass.

To measure DCB-extractable Fe and Al, 30 ml of citrate-bicarbonate solution, containing 26.7 ml of 0.4 M $Na_3C_6H_5O_7.2H_2O$ and 3.3 ml of 0.67 M $NaHCO_3$, was added to the 1 g of aggregated and disaggregated sample and 10 ml of deionized water in each tube. The tubes were then placed in a water bath. The

final concentrations of citrate and bicarbonate were 0.27 M and 0.055 M, respectively. When the temperature in the tubes was at 75 °C, sodium dithionite was added in three 0.3-g portions at 5 min intervals (Mehra and Jackson, 1958). After 15 min at temperatures between 75 and 80 °C, the samples were removed from the water bath, cooled, centrifuged at 1500 rpm for 5 min, and weighed. The supernatant was decanted and saved for Fe and Al measurements. The tubes were reweighed to measure the mass of entrained solution from this first extraction. Then, 40 ml of citrate-bicarbonate solution (0.27 M Na-citrate and 0.055 M Na-bicarbonate) was added to each tube, and the samples were sequentially extracted a second time with DCB, using the same procedure as for the first extraction. Two more extractions, for a total of four, were done on each aggregate size sample. The supernatant solutions for each successive extraction were kept separate so that the effect of each extraction could be measured. Iron and Al were measured by atomic absorption using air-acetylene and N$_2$O-acetylene as oxidizers, respectively. Standards were prepared with the same background solutions used in the extractions. Supernatant solutions were diluted when necessary. Entrained solution was corrected in the cumulative extraction calculations. Calculations of Fe and Al concentrations in each extraction were done as follows:

$$Fe_1 \ (\text{g kg-1 aggregates}) = C_1 \times V_1 / M_{aggr} \tag{2.2}$$

$$Fe_2 = Fe_1 + [C_2 \times (V_{1entr} + V_2) - C_1 \times V_{1entr}] / M_{aggr} \tag{2.3}$$

etc.

where Fe_i (or Al_i) is the amount of Fe (or Al) C_i and V_i are solution concentration and added solution volume in the ith extraction, M_{aggr} is aggregate mass, and $V_{i\text{-}entr}$ is the volume (mass) of entrained solution remaining in the tubes after the ith extraction.

Other Chemical and Mineralogical Analyses

Total carbon was measured in triplicate in the aggregate samples by high-temperature combustion at 900 °C using a Dohrmann DC-190 high-temperature TOC analyzer with a boat sampler. Because the soils contain no inorganic C, total C is equal to organic C.

X-ray diffraction and differential thermal analysis were used to quantify minerals in the clay fraction of each aggregate size sample as will be described below. Samples of each aggregate size fraction were treated with H_2O_2 to oxidize organic matter and dispersed by sonicating. The clay ($< 2\mu m$) was then separated by sedimentation. After the clay fraction was separated, NaCl was added to the suspension to promote flocculation of the clay separate. The clay separate was then placed in dialysis tubing to eliminate NaCl. The salt-free suspension was freeze-dried and saved for mineralogical analyses.

To concentrate Fe oxides in the clay fraction for x-ray diffraction quantification of hematite and goethite (Kämpf and Schwertman, 1982a), 5 g of the clay fraction of each aggregate size was placed in teflon beakers, and 100 ml of 5 M NaOH was added. The beakers were placed in a sand-bath and boiled for 1 h. The suspension was then cooled, transferred to 250-ml centrifuge tubes, and centrifuged at 1500 rpm for 5 min. After the supernatant solution was decanted, the material left in the centrifuge tubes was washed once with 100 ml of 5 M NaOH, once with 0.5 M HCl to dissolve sodalite, twice with 1 N $(NH_4)_2CO_3$ to remove NaCl, and twice with deionized water to remove NH_4 and CO_3. The samples were transferred to glass beakers and dryed overnight to volatilize the remaining $(NH_4)_2CO_3$ (Kämpf and Schwertman, 1982b).

To quantify the hematite:goethite ratio in the NaOH-treated clay fraction of each aggregate sample, the integrated intensities (peak areas) of hematite (012) peaks at 0.369 nm and goethite (110) peak at 0.413 nm (Kämpf and Schwertmann,

1982a) were measured on random powder samples and compared with the peak ratios for hematite and goethite standard mixtures (Appendix A2). The standards were prepared by mixing reagent-grade Fe_2O_3 and synthetic goethite (Atkinson, 1968) in a mortar and pestle for Hm/(Hm+Gt) ratios from 0 to 0.6. The same amount of material from each sample and standard (0.4 g) was poured onto a piece of filter paper in the cavity of an XRD specimen holder, to give a constant packing density for all samples and standards. Each specimen was x-rayed with Cu-Kα radiation from 20 to 40 °2θ in 0.01 °2θ steps, 3 sec per step, using a Philips APD 3270 diffractometer equipped with a Ni filter. This instrument also has a monochromator between the specimen and detector, which minimizes the Fe fluorescence intensity at the detector. After each sample or standard was x-rayed once, it was removed from the sample holder, remixed, put back into the sample holder, and x-rayed again. This procedure was repeated so that total of three x-ray diffractograms were obtained for each sample and standard. The average of the integrated peak areas for the three diffractograms was used to calculate the Hm/(Hm+Gt) ratio in each sample.

The Hm/(Hm+Gt) ratio in the NaOH-treated clay fraction was converted into hematite and goethite concentrations in the aggregate samples by assuming that the aggregates had the same Hm/(Hm+Gt) ratio as the NaOH-treated clay fraction, that hematite and goethite were the only crystalline Fe oxides present, and by equating the difference between dithionite-extractable Fe (Fe_d) and oxalate-extractable Fe (Fe_o) with crystalline Fe oxides, a widely accepted operational definition. The former assumption is justified because hematite and goethite were the only crystalline Fe oxides detected by x-ray defraction (Appendix A3). Hematite and goethite concentrations in each aggregate sample were calculated with the equations:

$$\text{Hm (g kg}^{-1}\text{ aggregates)} = \text{Hm/(Hm+Gt)} \times (Fe_d - Fe_o) \qquad (2.4)$$

$$Gt \ (g \ kg^{-1} \ aggregates) = [1 - Hm/(Hm+Gt)] \ x \ (Fe_d-Fe_o) \qquad (2.5)$$

Kaolinite and gibbsite were quantified by differential thermal analyses (DTA) in the dried clay fraction that had been treated with DCB to remove Fe oxides. The integrated area of endothermic peaks of gibbsite (350 °C) and kaolinite (550 °C) were compared to the same peak areas obtained from standards prepared with natural kaolinite and α-Al(OH)$_3$ reagent.

Statistical Analyses

To determine whether each of the soil properties described above differs with aggregate size, the triplicate physical, chemical, and mineralogical analyses were statistically analyzed using a two-factor split-plot ANOVA. The four soil samples (A and B horizons of the Yellow-Red and Dark-Red Latosols) were the main factor which was split into two aggregate sizes as the second factor. The least significant difference (LSD) for each property was calculated for $\alpha = 0.05$ and $\alpha = 0.01$.

Results and Discussion

Effect of Aggregate Size on Particle Size Distribution

The amount of total clay of A-horizon aggregates was significantly greater in large than small aggregates, whereas the smaller aggregates contained more sand than did the large aggregates (Table 2.1). The higher sand content of the small aggregates may indicate that some of the material included as small "aggregates" may actually have been fine or even very fine sand particles that were released when larger aggregates ruptured. Even if this is the case, the high clay plus silt contents (greater than about 85 %) indicate that the material in each aggregate size class is composed mainly of true aggregates.

Table 2.1. Particle size distribution of two aggregate size fractions of A and B horizons of Yellow-Red and Dark-Red Latosols.

Horiz	Aggr Size	Clay	Silt	Sand
		——— g (kg aggregate)$^{-1}$ ———		
	Yellow-Red Latosol			
A	1 - 2 mm	740ab	162bc	97b
	0.1 - 0.2 mm	658c	177b	164a
B	1 - 2 mm	729ab	177b	94b
	0.1 - 0.2 mm	706b	203a	90b
	Dark-Red Latosol			
A	1 - 2 mm	708b	184ab	108b
	0.1 - 0.2 mm	659c	172b	169a
B	1 - 2 mm	752a	139cd	108b
	0.1 - 0.2 mm	755a	133d	112b
LSD	$\alpha = 0.01$	41	26	21
	$\alpha = 0.05$	28	18	15

Numbers followed by the same letter are not statistically different at $\alpha=0.01$.

For B horizon samples, neither clay nor sand concentration differ with aggregate size. The absence of an increase in sand content with a decrease in aggregate size indicates that larger aggregates did not rupture and release sand that was collected on the 0.125-mm sieve. Thus, either the B-horizon aggregates are more stable than A-horizon aggregates, or their particle-size distribution is more uniform in different aggregate sizes.

Effect of Aggregation on Extraction of Al and Fe

Oxalate extractions: Aggregation had a fairly small effect on concentrations of oxalate-extractable Fe (Figure 2.1) and Al (Figure 2.2). Disaggregation generally increased the amount of Fe and Al extracted by oxalate in the large aggregates from all four soil horizons. For the small aggregates, disaggregation caused a small increase (not statistically significant) in oxalate-extractable Fe and Al, but the effect was smaller for the B than A horizon aggregates. Thus, aggregation had a greater effect on oxalate-extractable Fe and Al in large than small aggregates because the reaction is more transport-limited in large than in small aggregates. An alternative explanation for the greater effect of aggregation for large than small aggregates may be that small aggregates are so stable that sonication does not effectively disaggregate them. Evidence against the latter explanation will be provided by the DCB extraction results. Clearly, the ability of oxalate to extract Al and Fe from aggregated materials is transport-limited and depends on both aggregate size and aggregate composition. The results for disaggregated samples, which are not transport-limited, provide a better estimate of the true amount of oxalate extractable Fe and Al and therefore are reported in Table 2.2. The effect of aggregate size on Fe and Al extracted from disaggregated samples will be discussed below.
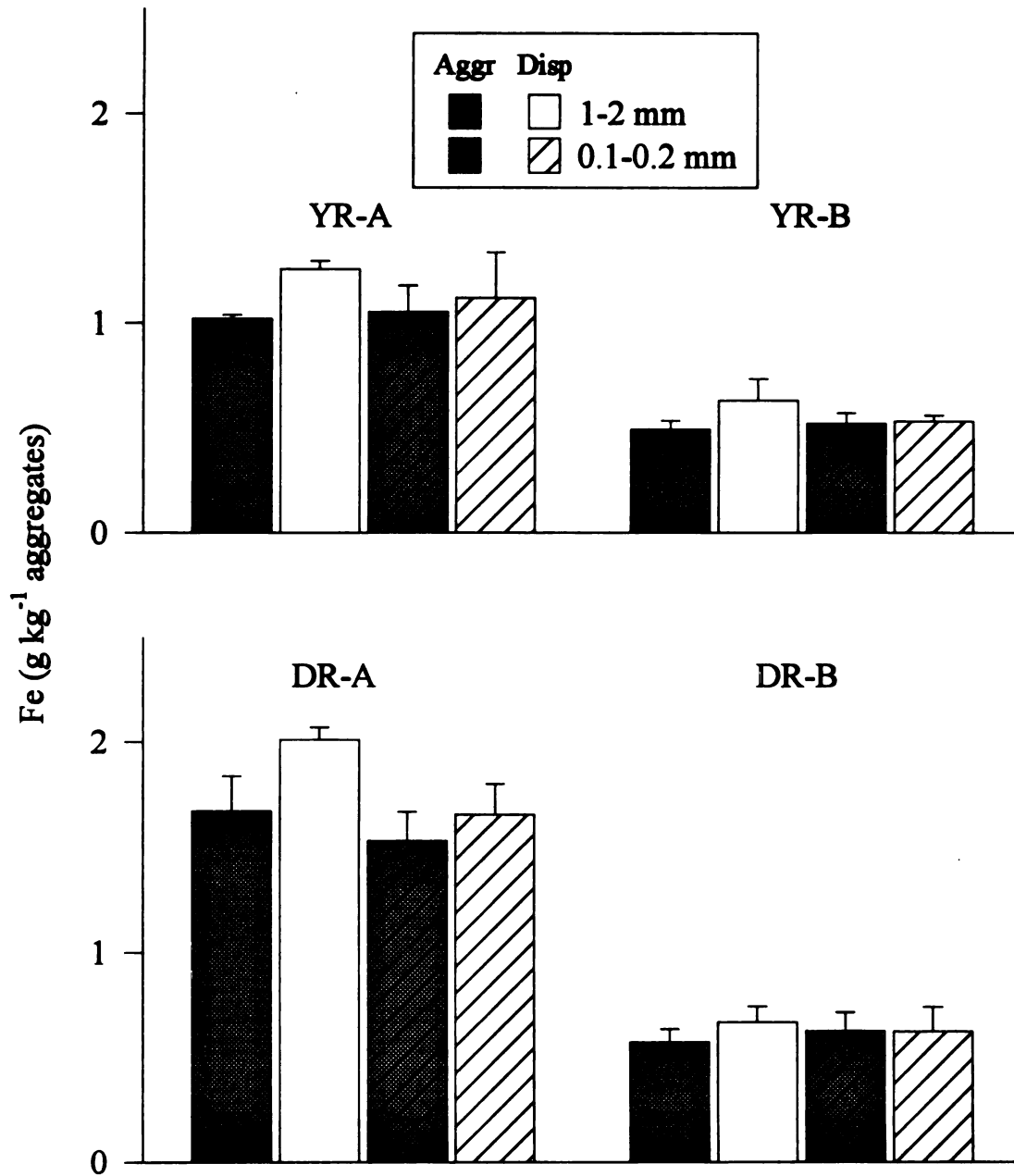
Figure 2.1. Effect of aggregation and aggregate size on the amount of Fe extracted by acid ammonium oxalate. Error bars represent the standard deviation of triplicate samples.
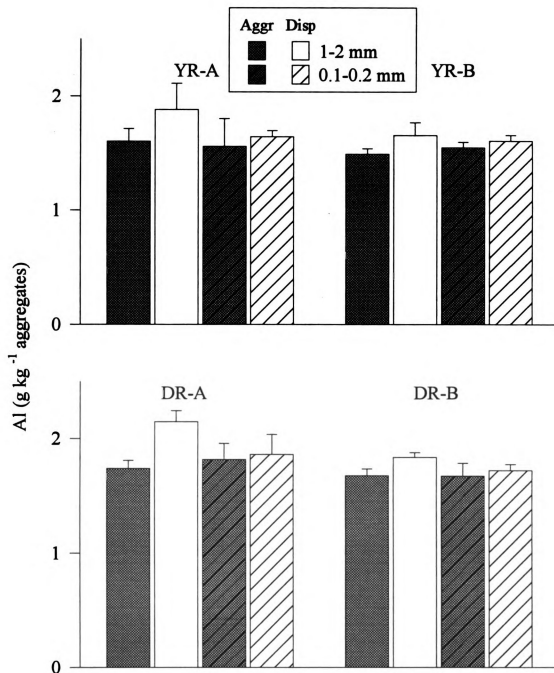
Figure 2.2. Effect of aggregation and aggregate size on the amount of Al extracted by the acid ammonium oxalate. Error bars represent the standard deviation of triplicate samples.

Table 2.2. Chemical and mineralogical properties of two aggregate size fractions of A and B horizons of two Oxisols from Brazil (triplicate analysis).

Horiz	Aggr Size	Carb	Fe$_o$	Al$_o$	Fe$_d$	Al$_d$	Fe$_o$/Fe$_d$	Hm	Gt	Hm/Gt	Gb	Kt
			g (kg aggregate)$^{-1}$					g (kg aggr)$^{-1}$			g (kg aggr)$^{-1}$	
			Yellow-Red Latosol									
A	1 - 2 mm	15.1*ab*	1.25*c*	1.87*b*	104*b*	30*ab*	0.012*b*	14*e*	149*bc*	0.094*e*	270	340
	0.1 - 0.2 mm	17.2*a*	1.11*d*	1.64*cd*	94*c*	27*c*	0.012*b*	15*e*	132*d*	0.115*d*	260	350
B	1 - 2 mm	9.7*c*	0.63*ef*	1.65*cd*	114*a*	30*ab*	0.005*c*	18*d*	159*a*	0.119*d*	290	340
	0.1 - 0.2 mm	8.4*c*	0.53*f*	1.60*d*	113*a*	31*ab*	0.004*c*	20*d*	156*ab*	0.131*d*	280	360
			Dark-Red Latosol									
A	1 - 2 mm	18.5*a*	2.01*a*	2.14*a*	103*b*	32*a*	0.019*a*	24*c*	133*d*	0.188*c*	350	240
	0.1 - 0.2 mm	19.5*a*	1.65*b*	1.86*b*	92*c*	29*bc*	0.018*a*	27*b*	113*e*	0.242*b*	350	240
B	1 - 2 mm	11.1*bc*	0.66*e*	1.83*b*	115*a*	32*a*	0.005*c*	34*a*	144*c*	0.239*b*	390	260
	0.1 - 0.2 mm	10.8*bc*	0.62*ef*	1.72*c*	112*a*	30*ab*	0.005*c*	36*a*	136*d*	0.268*a*	370	270
LSD: α = 0.01		4.8	0.12	0.11	7.0	2.3	0.004	2.7	7.0	0.020	¶	¶
0.05		3.3	0.09	0.09	4.8	1.8	0.003	1.9	4.8	0.014	¶	¶

Numbers followed by the same letter are not statistically different at P < 0.01.

¶ No replicates in the measurements to allow statistical parameters.

Fe$_o$ and Al$_o$: Fe and Al extracted by acid ammonium oxalate; Fe$_d$ and Al$_d$: Fe and Al extracted by dithionite–citrate–bicarbonate (DCB);

Hm: hematite; Gt: goethite; Gb: gibbsite; Kt: kaolinite.

Dithionite Extractions: Aggregation had a large effect on the concentrations of Fe (Figure 2.3) and Al (Figure 2.4) sequentially extracted by DCB. For B-horizon samples, the first DCB treatment extracted about three times more Fe and Al from disaggregated than aggregated samples. For A-horizon samples, disaggregation caused only a two-fold increase in the Fe and Al concentrations extracted with the first DCB treatment. The difference between aggregated and disaggregated samples decreased with each successive DCB extraction, although even after four extractions the cumulative Fe and Al concentrations generally were still greater in disaggregated than aggregated samples. The one exception was DCB-extractable Fe in the small A-horizon aggregates (Figure 2.3). For these small A-horizon aggregates, the lower clay content and higher sand content (Table 2.1) may have both caused these aggregates to have less Fe oxides, and caused aggregation to be slightly less important than for the other aggregate samples. Disaggregation had approximately the same effect in large and small aggregates. Thus, there was no evidence that small aggregates are more resistant to sonication than are large aggregates.

For disaggregated samples, cumulative DCB-extractable Fe and Al did not reach a plateau until the second or third extraction. Dithionite was not limiting these extractions, so this result indicates that sonication in deionized water may not cause complete dispersion, and that each successive DCB treatment probably caused additional disaggregation and allowed more Fe and Al oxides to come into contact with citrate and dithionite. The first DCB treatment extracted relatively less Fe and Al from A than B horizons, whereas the second DCB treatment extracted relatively more from A than B horizons (Figures 2.3 and 2.4). The relative ineffectiveness of the first DCB extraction on A-horizon samples might suggest that sonication causes greater dispersion in B than A horizons, but this
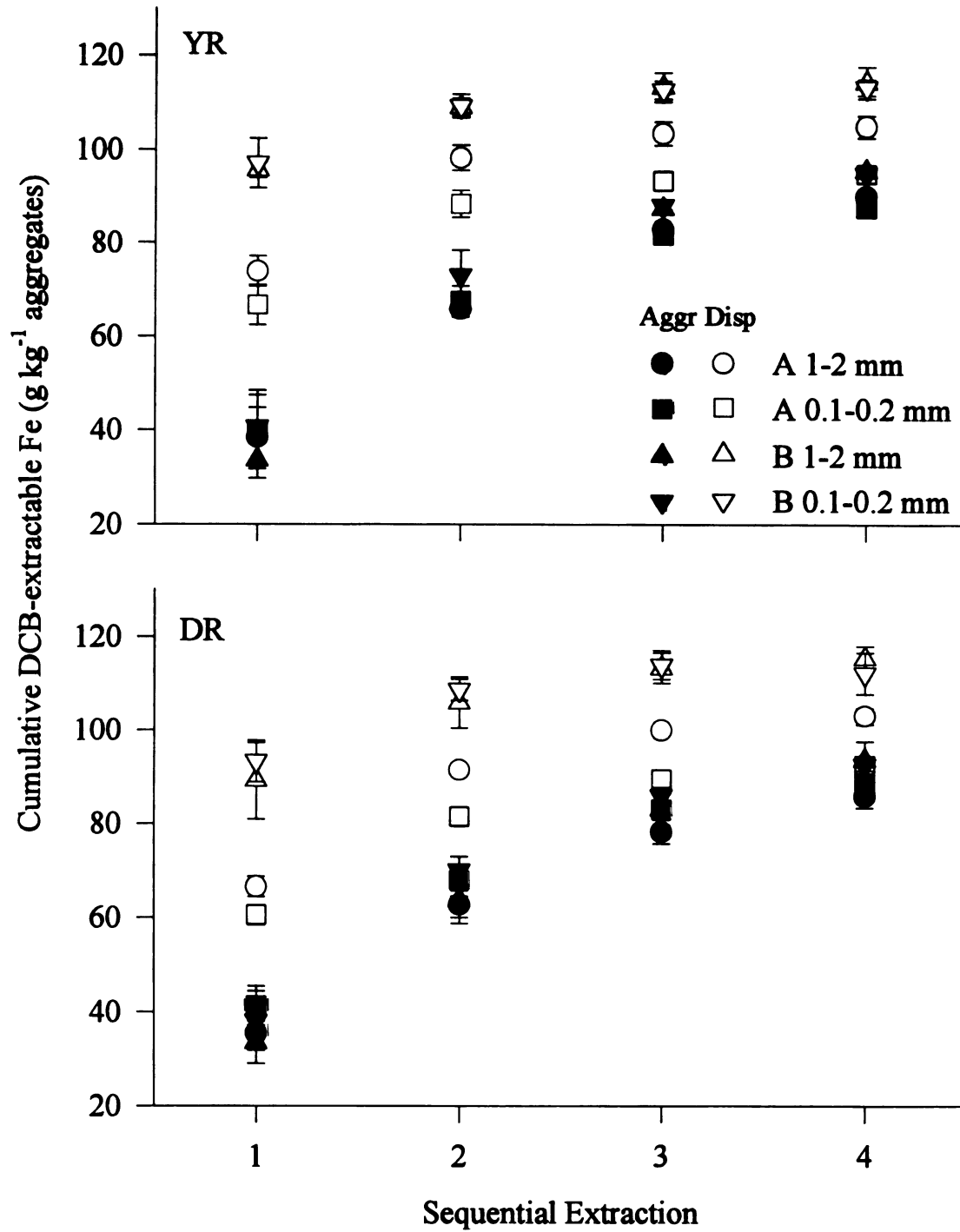
Figure 2.3. Effect of aggregation and aggregate size on DCB-extractable Fe. Error bars represent the standard deviation of triplicate samples.
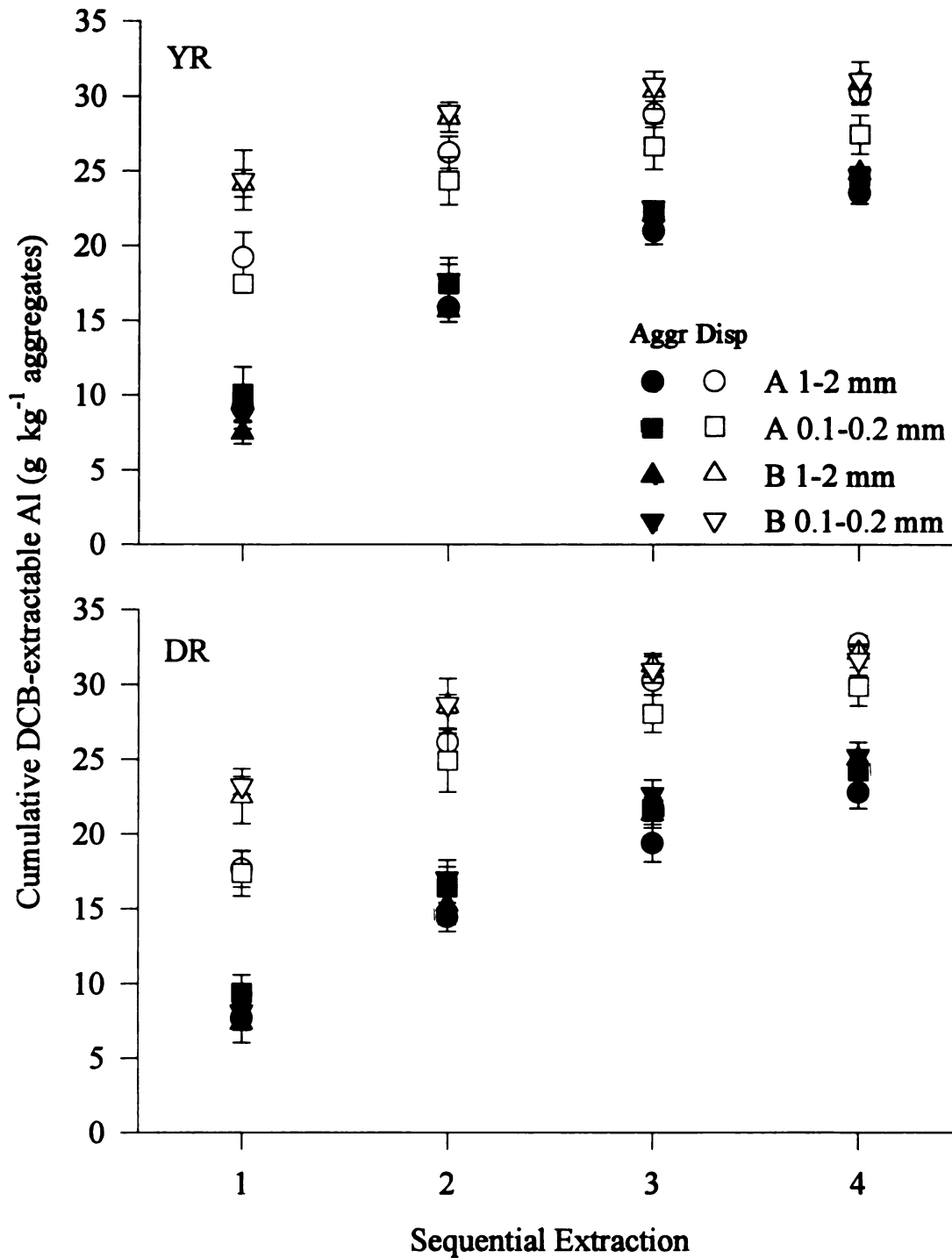
Figure 2.4. Effect of aggregation and aggregate size on DCB-extractable Al. Error bars represent the standard deviation of triplicate samples.

interpretation is dubious because sonication had greater effect on A than B horizon samples during the oxalate extractions (Figures 2.1 and 2.2). Alternatively, the relative ineffectiveness of the first DCB treatment for A horizon samples may be caused by the strong complexation of Fe and Al by solid-phase soil organic matter, such that the Fe and Al are not readily released to solution and thus are not detected by atomic absorption.

The difference between aggregated and disaggregated samples (Figures 2.3 and 2.4) clearly show that DCB extractions are transport-limited in aggregated samples. Even after four extractions, the results for aggregated samples do not reflect true dithionite-extractable Fe and Al; more than four extractions are apparently needed to release all "free" Fe oxides from aggregates. Thus, cumulative Fe and Al extracted by four DCB extractions in disaggregated samples are considered the true DCB-extracted concentrations (Table 2.2) and will be used below to evaluate the effect of aggregate size on composition.

Effect of Aggregate Size on Chemical and Mineralogical Composition

Within each soil and horizon, aggregate size did not have an effect on organic carbon (Table 2.2). This result contradicts the hypothesis that organic carbon should be higher in large aggregates because large aggregates are composed of small aggregates bound together mainly by organic carbon. Although the effect of aggregate size was not significant (at $\alpha = 0.01$), B-horizon samples showed the expected trend of nominally higher organic carbon in large aggregates, whereas the opposite was true for A horizon samples.

The concentrations of Fe and Al extracted by oxalate and by DCB from previously sonicated A horizon aggregates were always greater for large than small aggregates (Table 2.2). For B horizon samples, however, the effect of aggregate size generally was not significant at $\alpha = 0.01$ (Table 2.2). The reason for the greater dependence on aggregate size in A than B horizons is not known. Because

both oxalate-extracted Fe (Fe_o) and dithionite-extracted Fe (Fe_d) were greater in large than small aggregates, aggregate size had no effect on Fe_o/Fe_d. As expected, based on the higher organic carbon content of the A horizons, the Fe_o/Fe_d ratio was about three times greater for A than B horizon aggregates.

For all horizons and soils, hematite concentrations were nominally greater in small than large aggregates, though the difference was only significant (at $\alpha = 0.01$) for A horizon of the DR soil (Table 2.2). In contrast, goethite concentrations were significantly higher in large than small aggregates. Consequently, Hm/Gt ratios were higher in the small than large aggregates. Gibbsite and kaolinite do not appear to vary with aggregate size, though only one sample from each dispersed clay sample was analyzed by DTA.

Conclusions

Aggregation greatly inhibited extraction of Fe and Al from both large (1 to 2 mm) and small (0.125 to 0.25 mm) aggregates in Oxisols. Consequently, chemical analyses on samples that previously have been disaggregated by sonication provide more accurate information about aggregate composition than do analyses of untreated aggregates. For the Yellow-Red (Una Variant) and Dark-Red Latosol aggregates used in this study, the composition of the large aggregates differs from the composition of the small aggregates. Specifically, concentrations of oxalate-extractable and DCB-extractable Fe and Al, as well as goethite, are all higher in large than small aggregates. Total clay contents were higher in large than small aggregates. The effect of aggregate size on composition was much more important for A than B horizon aggregates. The results of this study suggest that aggregate stability and P sorption, both which depend strongly on the concentration and type of Fe oxides, are likely to differ between large and small aggregates. Furthermore, aggregation is likely to greatly inhibit P sorption kinetics, particularly for large aggregates, just as aggregation greatly inhibited reductive dissolution of Fe during DCB extractions.

Bibliography

Arduino, E., E. Barberis, and V. Boero. 1989. Iron oxides and particle aggregation in B horizons of some Italian soils. Geoderma. 45:319-329.

Atkinson, R.J., A.M. Posner, and J.P. Quirk, 1968. Crystal nucleation in Fe(III) solutions and hydroxide gels. J. Inorg. Nucl. Chem. 30:2371-2381.

Barberis, E., F.A. Marsan, V. Boero, and E. Arduino. 1991. Aggregation of soil particles by iron oxides in various size fractions of soil horizons. J. Soil Sci. 42:535-542.

Fontes, M.P.F. 1992. Iron oxide-clay mineral association in Brazilian Oxisols: a magnetic separation study. Clays and Clay Miner. 40:175-179.

Giovannini, G., and P. Sequi. 1976. Iron and aluminum as cementing substances of soil aggregates. II. Changes in stability of soil aggregates following extraction of iron and aluminum by acetylacetone in a non-polar solvent. J. Soil Science 27:148-153.

Kämpf, N., and U. Schwertmann. 1982a. Quantitative determination of goethite and hematite in kaolinitic soils by x-ray diffraction. Clay Miner. 17:359-363.

Kämpf, N., and U. Schwertmann. 1982b. The 5-M-NaOH concentration treatment for iron oxides in soils. Clays and Clay Miner. 30:401-408.

Mehra, O.P., and M.L. Jackson. 1958. Iron oxide removal from soils and clays by a dithionite-citrate system buffered with sodium bicarbonate. Clays and Clay Miner. 7:317-327.

Moura Filho, W., and S.W. Buol. 1976. Studies of a Latosol Roxo (Eutrorthox) in Brazil: micromorphology effect on ion release. Experientiae. 21:161-177.

Resende, M. 1976. Mineralogy, chemistry, morphology and geomorphology of some soils of the Central Plateau of Brazil. West Lafayette: Purdue University, 218p. (Ph. D. Dissertation)

Santos, M.C.D., A.R. Mermut, and M.R. Ribeiro. 1989. Submicroscopy of clay
    microaggregates in an Oxisol from Pernambuco, Brazil. Soil Sci. Soc. Am. J.
    53:1895-1901.

Schwertmann, U. 1964. Differenzierung der eisenoxide des bondes durch
    extraktion mit ammonium-oxalat-losung. Zeitschrift fuer Pflanzenernahrung.
    105:194-202.

Schwertmann, U., and N. Kämpf. 1985. Properties of goethite and hematite in
    kaolinitic soils   of Southern and Central Brazil. Soil Sci. 139:344-350.

Tisdall, J.M., and J.M. Oades. 1982. Organic matter and water-stable aggregates in
    soils. J. Soil. Sci. 33:141-163.

United States Department of Agriculture, Soil Survey Laboratory Staff. 1992. Soil
    survey laboratory method manual. Soil Survey Investigation Report No. 42.
    400p.

Yoder, R.E. 1936. A direct method of aggregate analyses of soil and study of
    physical nature of erosion losses. J. Am. Soc. Agronomy, Madison, v.28,
    p.337-351.

Chapter 3

Phosphate-Induced Clay Dispersion as Affected by Aggregate Size and Composition in Oxisols

Abstract

High phosphate sorption and high stability of aggregates are characteristic of Oxisols. Phosphate sorbed in inner-sphere complexes brings negative charge to the surface of particles and thus can affect aggregate stability and clay dispersion. The objective of this research was to determine the effect of P sorption on clay dispersion from aggregates with different organic matter and hematite/goethite ratios. Aggregates of 1- to 2-mm and 0.125- to 0.25-mm diameter were fractionated from A and B horizons of two Oxisols, both with 165 g kg^{-1} Fe$_2$O$_3$, but which differ in hematite and goethite content. The effect of residual sorbed P (after sorption/desorption cycle in 0.015 M NaCl) on water dispersion of clay, and on electrophoretic mobility and isoelectric point (IEP) of dispersed clay was measured on all aggregate types. In B-horizon samples, phosphate sorption caused a decrease in IEP and caused the amount of dispersed clay to decrease, as IEP decreased to values closer to the pH of the soil suspension, decreasing net positive charge. Then, additional P sorption caused dispersed clay to increase, as IEP became lower than the pH of suspension and negative charge increased. In A horizons, P sorption had no effect on dispersed clay or on IEP of the dispersed clay. In both A and B horizons, dispersed clay ratios were much greater for large than small aggregates, although IEP was independent of aggregate size.

Introduction

Oxisols with medium to high iron content (greater than about 70 g kg^{-1}) in the clay fraction tend to contain small and very stable aggregates, especially in the B horizon (Resende et al., 1988; Fontes, 1992; Oliveira et al., 1992). A large number of studies have shown that Fe and Al oxides interact with clay minerals, particularly kaolinite (for a review, see Goldberg, 1989). Although most of these studies have used artificial oxides in laboratory, they strongly suggest that the interactions of Fe and Al oxides with each other and with other soil minerals are of fundamental importance for soil aggregation.

In soils, small aggregates (microaggregates) < 0.2 mm in diameter are composed of iron and aluminum oxides, clay, and organic matter, whereas larger aggregates are composed of microaggregates that are bound together mainly by organic matter and polyvalent metals (Giovanini and Sequi, 1976; Tisdall and Oades, 1982). There are some controversies about the role of iron oxides in soil aggregation. In Oxisols, the crystalline iron oxides goethite and hematite tend to form microaggregates among themselves, instead of interacting with kaolinite (Schwertmann and Kämpf, 1985). Such microaggregates of iron oxides, associated with organic matter and kaolinite, form larger aggregates in Oxisols (Santos, 1989). Magnetic separation data has provided additional evidence for interaction between iron oxides, kaolinite and gibbsite in Oxisols (Fontes, 1992). The fact that crystalline iron oxides tend to form microaggregates among themselves suggests that the observed interaction of iron oxides with other minerals in soils likely involves amorphous iron oxides, as amorphous oxides were observed to be very effective in aggregating soil particles (Arduino, et al., 1989; and Barberis et al., 1991), possibly because of the higher surface area and charge-per-unit-mass of amorphous oxides.

Most interactions involving iron oxides are pH-dependent, regardless of whether they interact among themselves or with other soil particles. The presence of net surface charge, either positive or negative, produces repulsive forces between like-charged particles and consequently reduces aggregate stability and increases clay dispersion (Gillman, 1974; Sumner, 1992). Aggregate stability decreases and clay dispersion increases as *net* surface charge increases. The surface-charge properties of Oxisols are determined by the concentration of iron and aluminum oxides, kaolinite, and organic matter, all of which cause surface charge in Oxisols to depend strongly upon pH. Iron and aluminum oxides bear *net* positive charge below pH 8-9 (Sposito, 1989a; 1989b; Stumm, 1992), although positively and negatively charged surface functional groups can coexist above and below the isoelectric point. Kaolinite has *net* negative charge above pH 4.5 (Ferris and Jepson, 1975; Sposito, 1989a; 1989b; Stumm, 1992), and organic matter is negatively charged at all soil pH.

Net surface charge is affected not only by mineralogy, organic matter concentration, and pH, but also by the sorption of ions that form inner-sphere complexes with surface functional groups (Hingston et al., 1972; van Raij and Peech, 1972; Wann and Uehara, 1978; Stumm, 1992). Specific (inner-sphere) sorption of anions decreases the *net* positive surface charge and thus shifts the isoelectric point (IEP, also known as the point of zero charge) to lower pH (Hingston et al., 1974; Sawhney, 1974; Wann and Uehara, 1978; Sposito 1989a; 1989b; Stumm, 1992). In positively charged soils, i.e., soils with pH<IEP, phosphate sorption should cause an increase in aggregate stability and a decrease in clay dispersion by making the soil less positive. Dispersed clay decreases as the quantity (IEP-pH) decreases in magnitude. However, if phosphate sorption is sufficient to give the soil *net* negative charge (i.e., shift the IEP such that pH>IEP) then additional phosphate sorption would cause an increase in clay dispersion.

Surface charge, P sorption, and aggregation clearly are all interdependent, and all are controlled by the composition of a soil material, more than by any other chemical or physical property. In Chapter 2, the composition of large (1- to 2 mm) Oxisol aggregates was shown to differ from that of small (0.125- to 0.25 mm) aggregates, especially in the A horizon. Large A horizon aggregates contain significantly more clay, goethite, and oxalate- and DCB-extractable Fe and Al than do A horizon microaggregates (at $\alpha = 0.01$). Based on their higher Fe and Al oxide concentrations, the larger aggregates of each horizon should be more stable than the microaggregates, at least prior to P sorption. In addition, the larger aggregates should sorb more P, because pH and organic matter are independent of aggregate size (Chapter 2). The effect of P sorption on aggregate stability and on the surface-charge properties and concentration of suspended clay for different aggregate sizes is more difficult to predict because of the complex relationship between composition, surface charge, and P sorption, and because the physical characteristics of the aggregates may also be important.

The objective of this research was to determine whether the concentration and surface charge properties of suspended clay, both before and after phosphate sorption, differ between large and small aggregates of A and B horizons of two Oxisols. To distinguish between the chemical effect of compositional differences and the physical effects of aggregation and aggregate size *per se*, the concentration and isoelectric point of suspended clay were measured both for aggregates and for samples that previously had been disaggregated by sonication.

Materials and Methods

Sample preparation and aggregate fractionation are described in Material and Methods section in Chapter 2. Relevant physical, chemical, and mineralogical properties of the aggregates are reported in Tables 2.1 and 2.2, and are described in detail also in Chapter 2.

Three grams of each size aggregates were placed in each of four 250-ml centrifuge bottles and pre-wetted with drops of deionized water. After wetting, 100 ml of deionized water was added to each tube. Half of the samples were sonicated at 100 Watts for 3 min to destroy the aggregates, and half of the samples were kept as aggregates. Next, 50 ml of 0.03 M NaCl was added to both aggregated and disaggregated samples, and the suspensions were adjusted to pH 5 with NaOH or HCl. The suspensions were shaken for five min and equilibrated overnight. The pH was readjusted to 5 where necessary. Then, 50 ml of solution containing 0, 15, 40, 80, or 150 mg L^{-1} P in 0.03 M NaCl was added to disaggregated and aggregated samples to give total initial P concentrations of 0, 0.12, 0.32, 0.64, and 1.2 mM (the ionic strength was 0.015 M). The suspensions were shaken for 48 h in a horizontal shaker at 200 rpm at 20 °C ± 2 °C in a constant-temperature chamber. A 48-h reaction time was chosen because the amount of phosphate sorbed after 48 h was greater than 90% of the total sorbed after 17 d (Chapter 4). Part of the aggregates in the unsonicated samples remained intact at the end of this shaking period, and part was dispersed and released clay into suspension. After the shaking period, suspension pHs were measured and the tubes were centrifuged for 5 min at 2000 rpm. The supernatant solutions were decanted and saved for P measurements, and each centrifuge bottle was weighed to determine the mass of entrained solution. Supernatant phosphate concentrations were measured using a Lachat flow-injection analyzer with the molybdenum blue-ascorbic acid reduction method of Murphy and Riley (1962). Sorbed P was calculated from the difference

between initial and final solution P concentrations and was expressed in mmol kg^{-1}:

$$Sorbed\ P = (P_{init} - P_{final})\ V\ /\ kg\ soil, \tag{3.1}$$

where P_{init} and P_{final} are the initial and final solution-phase P concentrations (mmol L^{-1}) and V is the solution volume.

For desorption measurements, the samples and entrained solution were shaken with 100 ml of 0.015 M NaCl for 24 h at 20 °C ± 2 °C, then centrifuged as before. The supernatant solutions were decanted and saved for P analyses. The bottles with soil and entrained solution were weighed to determine the mass of entrained solution. The amount of phosphate desorbed was calculated with the equation:

$$Desorbed\ P = [P_d\ (V_d + M_{entr}) - P_{final}\ M_{entr}]\ /\ kg\ soil, \tag{3.2}$$

where P_d is the P concentration in the desorption supernatant, V_d is the volume of NaCl solution added during desorption step, M_{entr} is the mass (= volume) of solution entrained after the sorption step, and P_{final} is defined above. The amount of phosphate remaining after desorption (residual P, mmol kg^{-1}) was calculated as the difference between sorbed and desorbed P.

To measure the effect of residual P on dispersible clay, the soil and entrained solution that remained in the bottles after desorption were transferred to 50-ml tubes, and the total volume (including entrained solution) was brought to 50 ml with deionized water and shaken overnight in an end-over-end shaker at 90 cycles per min. The tubes were removed from the shaker and shaken by hand for 30 sec in order to set time zero for settling clay-sized particles according to Stokes law. After 3 h of settling, 10-ml aliquots were withdrawn from the tubes at 4.5-cm depth and dried in weighed aluminum dishes for 24 h to determine the mass of dispersed clay-sized (< 2-μm) material. The method used for measuring dispersed

clay is similar to that suggested by Burt et al. (1993). After the 10-ml aliquot was taken for dispersed clay measurements, the pH of each suspension was measured in order to determine the difference between suspension pH and IEP (described below). To correct for different clay contents in different aggregate types, dispersed clay was expressed as a fraction of total clay. Total clay measurements were described in Chapter 2.

For electrophoretic mobility measurements, duplicate 0.1-ml aliquots of dispersed clay suspensions, with clay concentrations ranging from 80 to 150 mg L^{-1}, were transferred to 50-ml centrifuge tubes containing 40 ml of 0.015 M NaCl at pH 3, 5, 7, and 9. The pH of each clay suspension was measured, and approximately 30 ml of each suspension was placed into a Zeta Meter cell for electrophoretic mobility measurements. The voltage applied in the Zeta Meter was adjusted to give a measuring time of about 5 sec for each particle. A total of 15 to 30 particles was counted in the forward or reverse direction each time. Isoelectric point was determined graphically (visually) from plots of electrophoretic mobility vs pH (Appendix B1).

Results and Discussion

Phosphate sorption

Disaggregation generally had no effect on the amount of sorbed, desorbed, or residual P for the 48-h sorption time used in these experiments (Appendix B2). Thus, 48 h seems to be sufficient to overcome the physical effect of aggregation on P sorption, except in A-horizon microaggregates, where residual P at the highest initial P concentration was about 16 % greater for disaggregated samples than for untreated aggregates (Appendix B2). In contrast, disaggregation had a greater effect on Fe and Al extraction in large than small A horizon aggregates (Chapter 2). Because disaggregation did not affect P sorption for most of the samples and P

concentrations, only the results for untreated aggregates are shown in Figure 3.1 and discussed below.

In A-horizon samples, large aggregates sorbed more P than did microaggregates, except at the 0.12 mM initial P concentration, where aggregate size had no effect. The difference between large and small aggregates increased as the initial P concentration increased (Figure 3.1). Although both P sorption and residual P were greater in large aggregates than in microaggregates, the amount of P desorbed was independent of aggregate size. The higher residual P concentration in large than small aggregates can be accounted for by the higher clay (Table 2.1) and Fe and Al oxide contents of the large aggregates (Table 2.2). As the initial P concentration was increased from 0.64 to 1.2 mM, the amount of residual P in the small A horizon aggregates did not increase. This suggests that 0.64 mM initial P was enough to saturate the sites for inner-sphere phosphate sorption in these A horizon microaggregates. Additional phosphate that was sorbed at higher P concentration was easily desorbed, as shown by the increase in desorbed P (Figure 3.1).

In B horizon aggregates, aggregate size had a negligible effect on P sorption, desorption, and residual P, even at the highest initial P concentration used in this study (Figure 3.1). The lack of an aggregate-size effect in the B horizons of either soil is probably due to the very similar composition of large and small aggregates in the B horizon samples (Tables 2.1 and 2.2).

Aggregates from B horizons sorbed more and desorbed less P than did A-horizon aggregates. Thus, residual P, which represents "irreversibly" sorbed P in inner-sphere complexes, is greater in B than A horizons. High organic matter in the A horizon aggregates (Table 2.2) caused lower P sorption by making the A horizon material more negative and blocking some phosphate sorption sites. The
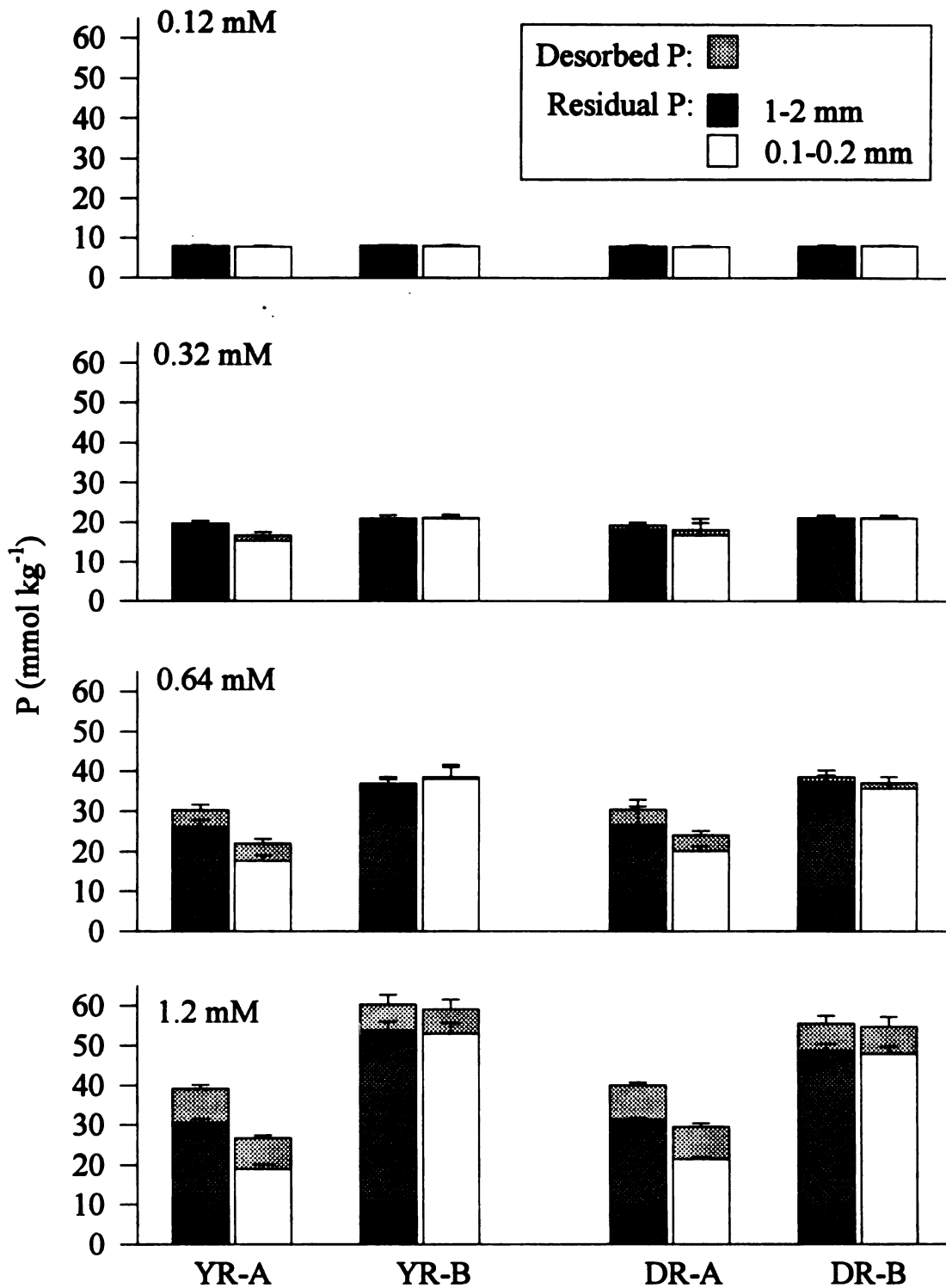
Figure 3.1. Effect of aggregate size on residual sorbed P (bottom bars),
desorbed P (upper bars), and total sorbed (combined bar height) at four
initial P concentrations for A and B horizons of Yellow-Red (YR) and
Dark-Red (DR) Latosols.
Average and standard deviation for duplicate samples.

greater desorption from A than B horizon aggregates suggests that A horizon sorbed more P in either outer-sphere or monodentate inner-sphere complexes, which are easier to desorb than bidentate inner-sphere complexes (Kafkafi, 1967; Hingston et al., 1974). All of the residual P resides in inner-sphere complexes (i.e., is specifically adsorbed), regardless of whether monodentate or bidentate.

For a given aggregate size, phosphate sorption by A horizon aggregates was nearly the same in the YR soil as in the DR soil, possibly because organic C content may limit P sorption in the A horizons of both soils, and both soils have similar OC concentrations, within the experimental error (Table 2.2). At the highest initial P concentration, B horizon aggregates of the YR soil sorbed significantly more P than did the B horizon of DR soil (Figure 3.1). This is in agreement with previous studies where soils higher in goethite relative to hematite sorb more P than soils with less goethite (Bigham et al., 1978; Curi and Franzmeier, 1984).

Effect of residual P on isoelectric point

Disaggregation had no effect on the IEP of suspended clay (Appendix B3), so only the results for aggregated samples are presented here. The effects of residual phosphate and aggregate size on the IEP of suspended clay are shown in Figure 3.2. At a given residual P concentration, aggregate size generally had no effect on IEP (Figure 3.2), although there is an effect of aggregate size for A horizon aggregates if IEP is plotted as a function of initial P (not shown).

In A-horizon samples, residual P had little effect on IEP of suspended clay, though IEP generally decreased slightly as residual P increased from 0 to 10 mmol kg^{-1} (Figure 3.2). Most of the P sorption in A horizon material may occur by displacing organic matter (Afif, 1995), so that phosphate sorption has little or no effect on IEP. Based on the small decrease in A horizon IEP at low residual P, it seems possible that a small amount of phosphate can sorb directly on oxides in A
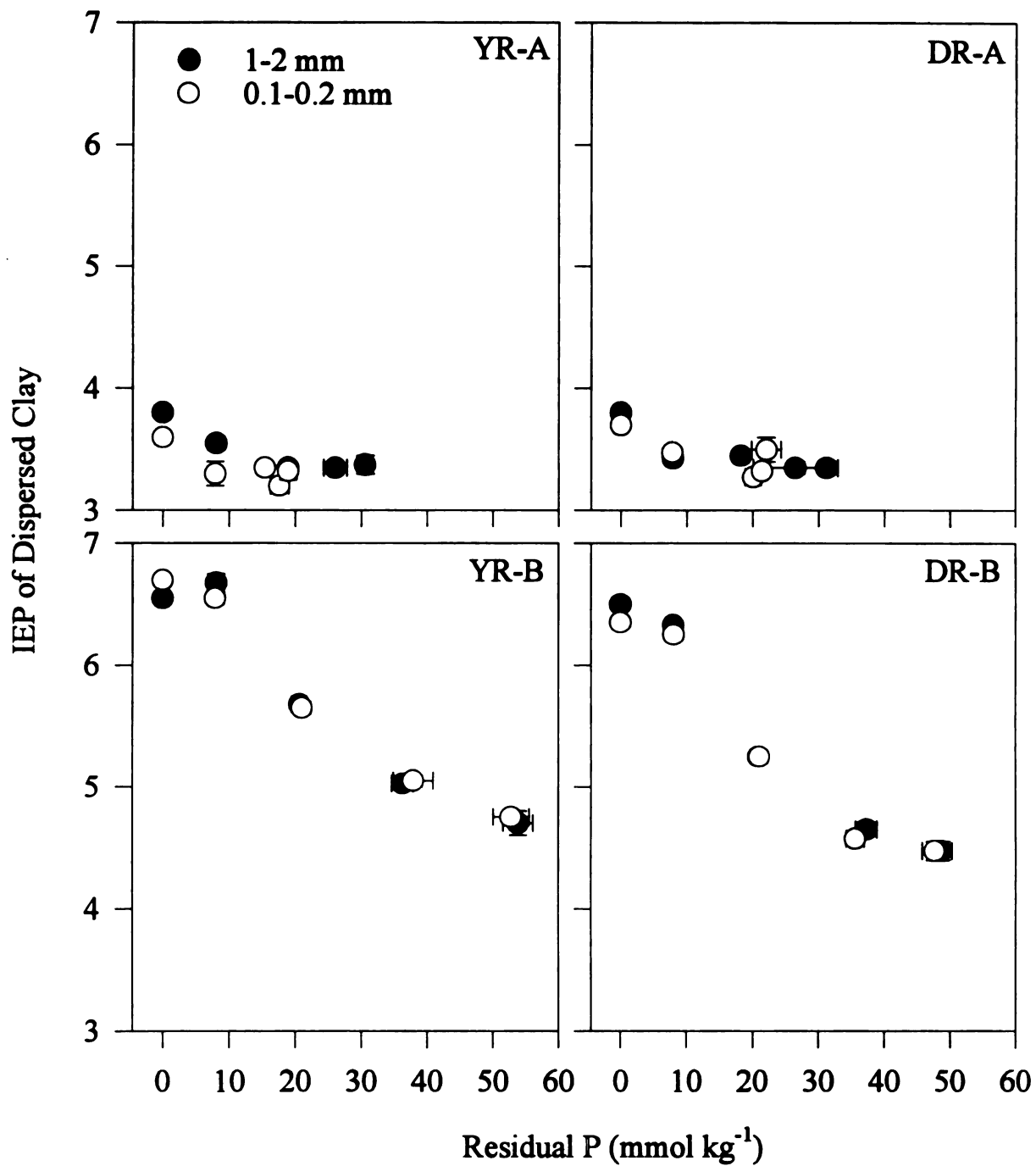
Figure 3.2. Effect of residual P and aggregate size on isoelectric points of dispersed clay from A and B horizons of Yellow-Red (YR) and Dark-Red (DR) Latosols. Average and standard deviation for duplicate samples.

horizons without displacing organic matter, and thereby increase the net negative charge and decrease IEP. The invariance in IEP with increasing residual P suggests that additional P is probably sorbed by ligand exchange with organic matter.

The IEP values at zero residual P in A horizons are much lower than in B horizon (Figure 3.2). Mainly the higher organic matter, and, to some extent, the lower iron oxide content (Table 2.2), are responsible for the lower IEP in A than B horizons. The IEPs at zero residual P (about 6.5 for B horizon and 3.7 for A horizon) show that prior to P sorption, B horizon aggregates were positively charged and A horizon aggregates negatively charged at the initial pH of 5. In B horizon samples, IEP decreased greatly with increasing residual P concentration (Figure 3.2). As negatively charged phosphate is sorbed by ligand exchange with OH or H_2O on surfaces of Fe and Al oxides, the net surface charge becomes less positive (more negative), and the IEP shifts to lower pH.

For A horizon samples, IEPs were the same for the YR soil as for the DR soil. As mentioned above for P sorption, the lack of a difference between the two soils for A-horizon samples may reflect the dominant effect of organic matter of A-horizon surface chemistry in Oxisols. For B horizon aggregates, the IEP of YR soil was initially somewhat higher than in the DR soil, though the difference may be within experimental error (Appendix B1). Over the entire range of P concentrations, the decrease in IEP was about the same for YR soil as for DR soil, even though the YR soil retained significantly more residual P (for 1.2 mM initial P) than did the DR soil. Thus, the decrease in IEP per mol of residual P (i.e., $\Delta IEP/\Delta P$) is less for the YR soil than the DR soil. The lower $\Delta IEP/\Delta P$ for the YR soil could possibly indicate that the higher goethite of this soil favors greater formation of bidentate rather than monodentate complexes. Bidentate complexes cause less negative charge than monodentate complexes (Hingston et al., 1974). Further research would be needed to verify this mechanistic interpretation of IEP results.

Effect of residual P on dispersed clay

The dependence of suspended clay concentration, expressed as a fraction of total clay (hereafter "clay ratio") on residual P is shown in Figure 3.3. Because disaggregation prior to P sorption had no effect on the clay ratio (Appendix B4), only the results for aggregated samples are shown here.

In A horizon samples, residual P had no effect on clay ratio (Figure 3.3), just as it had no effect on IEP (Figure 3.2). Small aggregates, which have higher Hm/Gt ratios (Table 2.2), seem to be more stable than large aggregates as shown by their lower clay ratio, regardless of whether the clay ratio is plotted as a function of residual P (Figure 3.3) or IEP-pH (Figure 3.4). The greater stability of small aggregates may suggest that even the slightly higher amounts of hematite in small than large aggregates promotes greater aggregate stability. A alternate explanation for the relative stability of microaggregates in the A horizons is that residual P was insufficient to promote clay dispersion. This latter explanation is not likely, however, because small aggregates also had lower clay ratio than large aggregates in the B horizons (Figure 3.3), where they had the same high residual P as large aggregates (Figure 3.1). The greater stability of small than large aggregates in both horizons of both soils contradicts our original hypotheses that large aggregates should be more stable due to their higher Fe and Al concentrations.

In the B horizon aggregates, the effect of residual P on clay ratio was very clear. The clay ratio decreased as the residual P increased to about 10 mmol kg^{-1}, then the clay ratio increased for values of residual P above 10 mmol kg^{-1} (Figure 3.3). The clay ratios of B-horizon aggregates at residual P higher than about 35 mmol kg^{-1} are similar to those ratios of the same size A-horizon aggregates at all amounts of residual P.

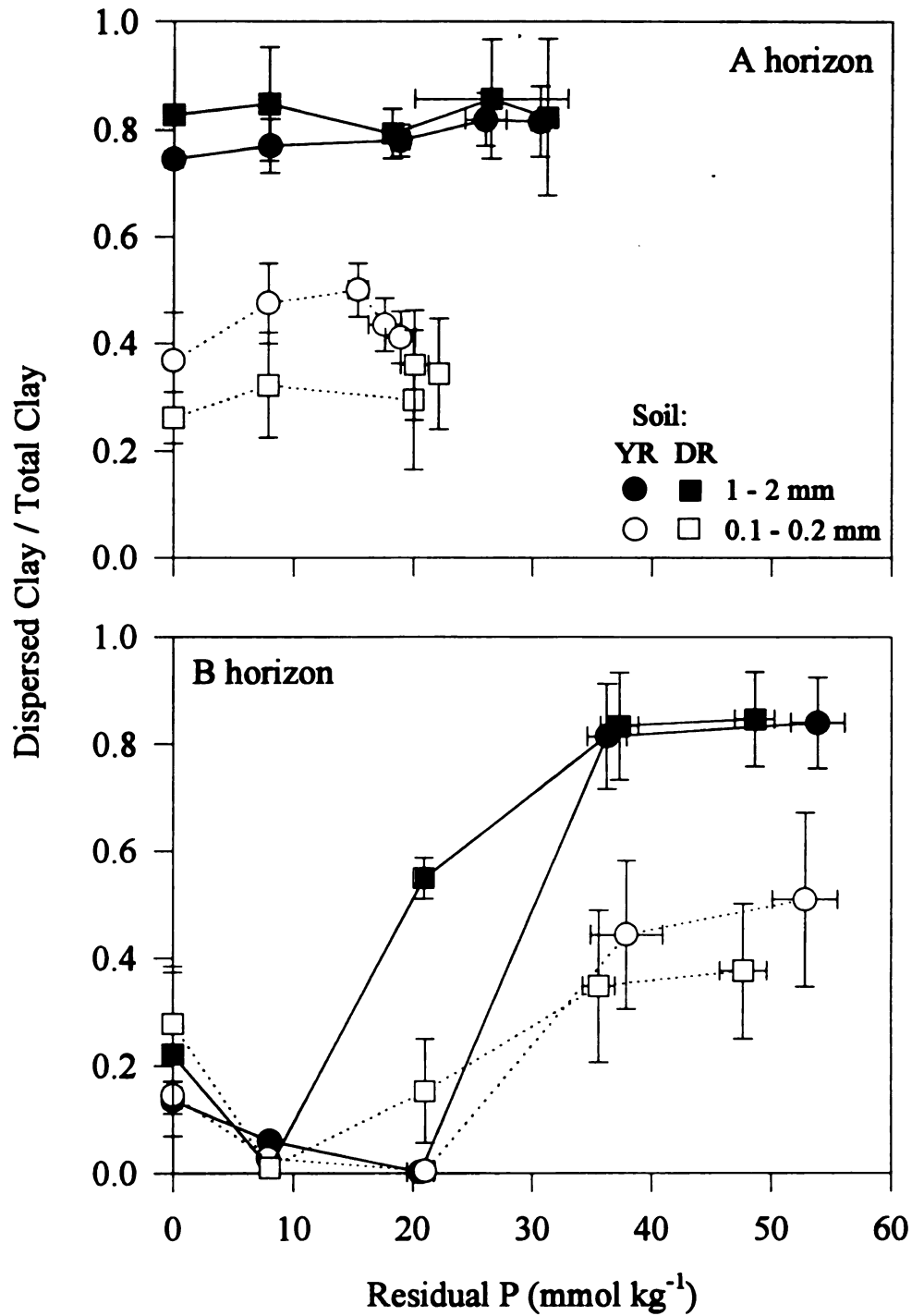Figure 3.3. Effect of residual sorbed P and aggregate size on dispersed/total clay for A and B horizons of Yellow-Red (YR) and Dark-Red (DR) Latosols. Average and standard deviation for duplicate samples.
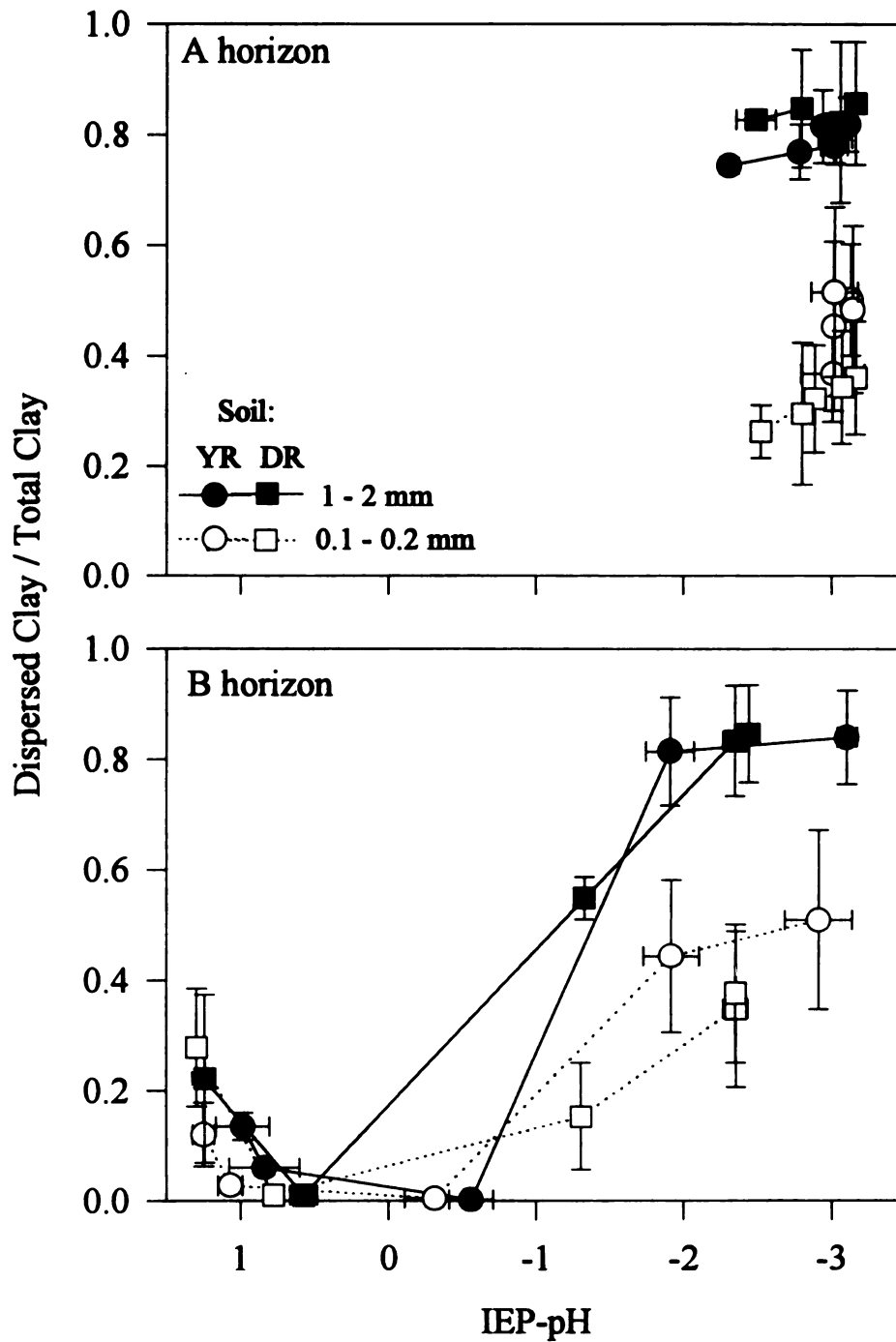
Figure 3.4. Effect of IEP-pH and aggregate size on dispersed/total clay for A and B horizons of Yellow-Red (YR) and Dark-Red (DR) Latosols. Average and standard deviation for duplicate samples.

Surprisingly, dispersed clay ratios were the same for the YR soil as for the DR soil, in spite of differences in Hm/Gt ratio. Thus, the greater Hm/Gt ratios of small than large aggregates is probably not the sole cause for their lower dispersed clay ratios.

Effect of Net charge on dispersed clay

When the clay ratio is plotted as a function of IEP-pH (Figure 3.4) the dispersed clay ratio is again much greater for large than small aggregates from both A and B horizons of both soils, but only when IEP-pH (which gives the sign and relative magnitude of surface charge) is negative. When IEP-pH for B-horizon samples is near zero, the dispersed clay ratios for both aggregate sizes are near zero. When IEP-pH ≥ 1, there is a very small or negligible effect of aggregate size on the dispersed clay ratio (Figure 3.4). Possible explanation for the effect of aggregate size on the dispersed clay ratio when IEP-pH < 0 will be discussed bellow.

The IEP values in the A horizon material were always 2 or 3 units below the suspension pH (Figure 3.4). Over this range of negative surface charge, the dispersed clay ratio for both aggregate sizes was essentially independent of IEP-pH, although there may be a very small decrease in dispersed clay ratio for the small aggregates as IEP-pH (surface charge) becomes less negative. For B-horizon samples, the clay dispersed ratio initially was at about 0.2 for both aggregate sizes when the soil was positively charged (IEP-pH ≈ 1) and little or no P was sorbed. As IEP-pH decreased to zero in response to phosphate sorption, dispersed clay decreased to zero, because aggregates were more stable and released less clay into suspension and because any clay released during shaking would flocculate rapidly. When B horizon samples sorbed enough P that surface charge (IEP-pH) was more negative, dispersed clay ratios increased markedly. When P sorption caused IEP-pH of B horizon aggregates to be negative, the dispersed clay ratio was much higher for large than small aggregates, just as noted above for negatively charged

A horizon samples. The results in Figure 3.4 show that the B horizon sorbed enough P to make it (or at least the clay dispersed from it) as negative as the A horizon, which derives its negative charge from organic matter. Another similarity between A and B horizon samples is that when IEP-pH < -2, the dispersed clay ratio seems to be independent of surface charge, at least for the YR soil. There is not enough data at low IEP-pH to determine whether such pattern also holds for the DR soil.

Perhaps the most striking feature of the dispersed clay ratios is that when the net surface charge is negative (IEP-pH < 0), the dispersed clay ratio at a given IEP-pH (i.e., same surface charge) is much greater for large than small aggregates, yet within a given aggregate size, the dispersed clay ratio is the same for A and B horizons and for the YR and DR soils. Thus, the aggregate size effect is not simply due to different surface charge in different aggregate sizes. Nor is it likely due to the slightly higher Hm/Gt ratio in small than large aggregates. If Hm/Gt ratio controls aggregate stability, the dispersed clay ratio should be lower in the DR soil, which has a higher Hm/Gt ratio, than in the YR soil, which has less hematite. Thus, the greater dispersed clay ratio for large aggregates must be related in A complex manner to the mechanism of aggregation as well as to aggregate composition.

Conclusions

The amount of residual P is smaller for small aggregates with higher organic matter and lower Fe and Al. However, the effect of residual P on IEP was independent of aggregate size. In both aggregate sizes, increasing residual P caused much greater decrease in IEP of B horizon than A horizon material.

Dispersion of clay was affected by residual P only in B horizon aggregates, not in A horizon aggregates. Small aggregates dispersed less (were more stable) than large aggregates. For a given aggregate size, the greater the difference between IEP and pH, in absolute value, the greater the amount of suspended clay, except when IEP-pH was less than -2. The difference in composition and mechanism of formation of small and large aggregates causes the small aggregates be more stable than large aggregates at a given IEP-pH value.

The results of this study indicate that phosphate has little effect on the surface chemistry of A horizon aggregates. Thus P fertilization may have a negligible effect on clay dispersion and subsequent erosion of A horizons, given that A horizons are already negatively charged prior to phosphate sorption. If phosphate leaches through the A horizon to the B horizon, P sorption can cause charge reversal and subsequent clay dispersion, though dispersed B horizon clay does not pose on erosion threat. Instead, dispersed B horizon oxides, along with sorbed P, may leach out of the soil and cause economic loss of nutrient P. Phosphate bound to dispersed B-horizon oxides may be quite mobile in the subsurface and may either pollute shallow groundwater or possibly reach surface water by baseflow.

Bibliography

Afif, E., V. Barron, and J. Torrent. 1995. Organic matter delays but not prevent phosphate sorption by cerrado soils from Brazil. Soil Sci. 159:207-211.

Arduino, E., E. Barberis, and V. Boero. 1989. Iron oxides and particle aggregation in B horizon of some Italian soils. Geoderma. 45:319-329.

Barberis, E., F.A. Marsan, V. Boero, and E. Arduino. 1991. Aggregation of soil particles by iron oxides in various size fractions of soil horizons. J. Soil Sci. 42:535-542.

Bigham, J.M., D.C. Golden, S.W. Buol, S.B. Weed, and L.H. Bowen. 1978. Iron oxide mineralogy of well-drained Ultisols and Oxisols: II. Influence on color, surface area, and phosphate retention. Soil Sci. Soc. Am. J. 42:825-830.

Burt, R., T.G. Reinsch, and W.P. Miller. 1993. A micro-pipette method for water dispersible clay. Commun. Soil Sci. Plant Anal. 24:2531-2544.

Curi, N., and D.P. Franzmeier. 1984. Toposequence of Oxisols from the Central Plateau of Brazil. Soil Sci. Soc. Am. J. 48:341-346.

Ferris, A.P., and W.P. Jepson. 1975. The exchange capacity of kaolinite and the preparation of homoionic clays. Journal of Colloid and Interface Science. 51:245-259.

Fontes, M.P.F. 1992. Iron oxide-clay mineral association in Brazilian Oxisols: a magnetic separation study. Clays and Clay Miner. 40:175-179.

Gillman, G.P. 1974. The influence of net charge on water dispersible clay and sorbed sulphate. Aust. J. Soil Res. 12:173-176.

Giovanini, G., and P. Sequi. 1976. Iron and aluminum as cementing substances of soil aggregates. II Changes in stability of soil aggregates following extraction of iron and aluminum by acetylacetone in a non-polar solvent. J. Soil Sci. 27:148-153.

Goldberg, S. 1989. Interaction of aluminum and iron oxides and clay minerals and their effect on soil physical properties: a review. Commun. Soil Sci. Plant Anal. 20:1181-1207.

Hingston, F.J., A.M. Posner, and J.P. Quirk. 1972. Anion adsorption by goethite and gibbsite. I The role of proton in determining adsorption envelopes. J. Soil Sci. 23:177-192.

Hingston, F.J., A.M. Posner, and J.P. Quirk. 1974. Anion adsorption by goethite and gibbsite. II: Desorption of anions from hydrous oxide surfaces. J. Soil Sci. 25:16-26.

Kafkafi, U., A.M. Posner, and J.P. Quirk. 1967. Desorption of phosphate from kaolinite. Soil Sci. Soc. Amer. Proc. 31:348-353.

Murphy, J., and J.P. Riley. 1962. A modified single solution method for determination of phosphate in natural waters. Analitica Chemica Acta. 27:31-36.

Oliveira, J.B., P.K.T. Jacomine, and M.N. Camargo. 1992. Classes gerais de solos do Brasil: guia auxiliar para reconhecimento. Jaboticabal, FUNEP. 201p.

Resende, M., N. Curi, and D.P. Santana. 1988. Pedologia e fertilidade do solo: interações e aplicações. Brasilia-DF, Brazil. MEC-ESAL-POTAFOS. 83p.

Santos, M.C.D., A.R. Mermut, and M.R. Ribeiro. 1989. Submicroscopy of clay microaggregates in Oxisol from Pernambuco, Brazil. Soil Sci. Soc. Am. J. 53:1895-1901.

Sawhney, B.L. 1974. Charge characteristics of soils as affected by phosphate sorption. Soil Sci. Soc. Am. Proc. 38:159-160.

Schwertmann, U., and N. Kämpf. 1985. Properties of goethite and hematite in kaolinitic soils of Southern and Central Brazil. Soil Sci. 139:344-350.

Sposito, G. 1989a. The chemistry of soils. New York, Oxford University Press. 277p.

Sposito, G. 1989b. Surface reactions in natural and aqueous colloidal systems. Chimia 43:169-176.

Se

S

Ti

Wa

an

Stumm, W. 1992. Chemistry of the solid-water interface: processes at the mineral-water and particle water interface in natural systems. New York, John Wiley and Sons, Inc. 428p.

Sumner, M.E. 1992. The electrical double layer and clay dispersion. In: Sumner, M.E., and B.A. Stewart. (ed) Soil crusting: chemical and physical processes. Boca Ranton, Fla. Lewes Publishers. 372p.

Tisdall, J.M., and J.M. Oades. 1982. Organic matter and water-stable aggregates in soils. J. Soil. Sci. 33:141-163.

Wann, S.S., and G. Uehara. 1978. Surface charge manipulation of constant surface potential soil colloids, I: Relation to sorbed phosphorus. Soil Sci. Soc. Am. J. 42:565-570.

van Raij, B., and M. Peech. 1972. Electrochemical properties of some Oxisols and Alfisols of the Tropics. Soil Sci. Soc. Am. Proc. 36:587-593.

Chapter 4

Kinetics of Phosphate Sorption Related to Aggregation, Aggregate Size, and Aggregate Composition in Oxisols

Abstract

Phosphate sorption in soils occurs in a fast step with displacement of OH and OH_2^+ groups, and a slow step that involves redistribution of the sorbed P throughout the surface and defects of minerals. Soil aggregates can affect the rate of phosphate sorption as it increases the distance to the sorption sites, so that sites become, at least for a while, unavailable, which affects especially the fast step of reaction. Such effect depend on stability and size of aggregates which are dependent on aggregate composition. The objectives of this research were to determine the effect of aggregate size, aggregate composition, and disaggregation on phosphate sorption kinetics in A and B horizons of two Oxisols which differ in Hm/Gt ratio. Large aggregates of A horizon sorbed more P than small aggregates. Disaggregation of the soil material prior to the sorption kinetics measurements increased the rate of P sorption, which shows that liquid-phase diffusion is rate limiting P sorption. The fast step of P sorption (before 8 min) was more affected by aggregation than was the slow step. The difference between aggregated and disaggregated samples decreases as time increased from 8 min to 1200 min (20 h).

Introduction

Phosphate sorption kinetics in Oxisols are important for soil fertility because the bioavailability of nutrient P depends on the relative rates of plant uptake vs. soil sorption. Phosphate sorption is closely related to the amount, type, and crystallinity of iron and aluminum oxides (Parfitt, 1978; 1989; Bigham et al., 1978; Curi and Franzmeier, 1984). Organic matter also can limit P sorption, mainly by competing with P for sorption sites on oxides (Sanyal et al., 1993; Afif et al., 1995). Iron and aluminum oxides and organic matter also promote aggregation (Chester et al., 1957; Arca and Weed, 1966, Giovanini and Sequi, 1976; Goldberg, 1989; Barberis et al., 1991), but the interrelationships between phosphate sorption kinetics, aggregation, and aggregate composition have not been studied thoroughly.

Phosphate sorption on hydrous metal oxides proceeds by a fast ligand-exchange reaction in which phosphate ions displace OH or OH_2^+ groups (Hingston et al., 1974; Parfitt, 1978), and a slow step that involves a solid-diffusion process. After the initial rapid sorption phase, further increases in P sorption with time are facilitated by redistribution of sorbed P into the particle interior by solid-state or surface diffusion (Bolan et al., 1985). Phosphate sorption in A-horizons may require ligand exchange of phosphate for organic matter, which slows the process (Afif et al., 1995). In soil aggregates, many sorption sites on constituent particles are "hidden" in the interiors of aggregates and thus are not readily accessible to bulk solution. Thus, even the fast ligand exchange reaction of phosphate sorption may be transport-limited in aggregated soils. Because aggregation increases the distance between bulk solution and sorption sites, phosphate sorption kinetics may be slower for large than small aggregates, particularly during the initial phase of phosphate sorption.

Laboratory studies with artificial iron oxide aggregates have shown that reaction kinetics depend upon both solid-phase (surface diffusion) on particle surfaces and liquid-phase diffusion in the pore spaces of iron oxide aggregates (Willet et al., 1988; Parfitt, 1989). Differences in aggregate and particle porosity cause differences in the accessibility of interior reactive sites and control the amounts of rapidly and slowly sorbed phosphate (Madrid and Aranbarri, 1985). Sollins (1991) has suggested that the physical characteristics of soil constituents may be very important in determining phosphate availability in acidic soils. In such soils, aggregating agents such as crystalline and amorphous oxides and organic matter differ in porosity. In addition, these aggregating agents probably are not uniformly distributed within an aggregate. Thus, the porosity and reaction kinetics of an aggregate will depend upon the relative proportions of organic matter, amorphous and crystalline oxides, as well as on the physical distribution of these constituents within an aggregate.

In soils, aggregation can make it difficult do distinguish between the chemical kinetics of a sorption reaction and the time-dependence of diffusion (Skopp, 1986). Such a distinction may be unnecessary if one is only interested in the reaction rate under a given set of conditions. However, to understand how changes in soil physical and chemical properties affect reaction rates, it is necessary to separate transport processes and chemical processes that affect reaction rates. Physical disaggregation or dispersion of soil aggregates, without altering chemical properties, can allow one to distinguish experimentally between physical and chemical rate-limiting process and to determine how these processes are affected by soil physical and chemical properties.

The objectives of this research were to determine the effect of aggregate size, aggregate composition, and disaggregation on P sorption kinetics at two initial P concentrations under varying temperature.

Materials and Methods

Soil sampling and aggregate fractionation are described in Chapter 2. Relevant physical, chemical, and mineralogical properties of the aggregates are reported in Tables 2.1 and 2.2, and described in detail also in Chapter 2.

Phosphate Sorption and Desorption

Three grams of each size aggregates were placed in each of four 250-ml centrifuge bottles and pre-wetted with drops of deionized water. After wetting, 100 ml of deionized water was added to each tube. Half of the samples were sonicated at 100 Watts for 3 min to destroy the aggregates, and half of the samples were kept as aggregates. Next, 50 ml of 0.03 M NaCl was added to both aggregated and disaggregated samples, and the suspensions were adjusted to pH 5 with NaOH or HCl. The suspensions were shaken for five min and let to equilibrate overnight. The pH was then readjusted to 5 where necessary. Then, 50 ml of solution containing 0, 15, 40, 80, or 150 mg L^{-1} P in 0.03 M NaCl was added to disaggregated and aggregated samples to give total initial P concentrations of 0, 0.12, 0.32, 0.64, and 1.2 mM (the ionic strength was 0.015 M). The suspensions were shaken for 48 h in a horizontal shaker at 200 rpm at 20 °C ± 2 °C in a constant-temperature chamber. A 48-h reaction time was chosen because the amount of phosphate sorbed after 48 h was greater than 90% of the total sorbed after 17 d. After the shaking period, the tubes were centrifuged for 5 min at 2000 rpm. The supernatant solutions were decanted and saved for P measurements, and each centrifuge bottle was weighed to determine the mass of entrained solution. The same procedure was done at 40 °C. Supernatant phosphate concentrations were measured using a Lachat flow-injection analyzer with the molybdenum blue-ascorbic acid reduction method of Murphy and Riley (1962). Sorbed P was calculated from the difference between initial and final solution P concentrations and was expressed in mmol kg^{-1}:

$$Sorbed\ P = (P_{init} - P_{final})\ V\ /\ kg\ soil, \tag{4.1}$$

where P_{init} and P_{final} are the initial and final solution-phase P concentrations ($mmol\ dm^{-3}$) and V is the solution volume.

For desorption measurements, the samples and entrained solution were shaken with 100 ml of 0.015 M NaCl for 24 h at 20 °C $\pm$ 2 °C, then centrifuged as before. The supernatant solutions were decanted and saved for P analyses. The bottles with soil and entrained solution were weighed to determine the mass of entrained solution. The amount of phosphate desorbed was calculated with the equation:

$$Desorbed\ P = [P_d\ (V_d + M_{entr}) - P_{final}\ M_{entr}]\ /\ kg\ soil, \tag{4.2}$$

where P_d is the P concentration in the desorption supernatant, V_d is the volume of NaCl solution added during desorption step, M_{entr} is the mass (= volume) of solution entrained after the sorption step, and P_{final} is defined above. Sorption and desorption maxima were calculated using the linear form of Langmuir equation:

$$P_{final}/Sorbed\ P = 1/kb + P_{final}/b \tag{4.3}$$

where b is capacity parameter (represents the maximum phosphate sorption), k is a constant related to adsorption energy, and P_{final} and $Sorbed\ P$ are defined above.

Both sorption maxima and desorption maxima were estimated using the b value of the equation.

Phosphate Sorption Kinetics

Phosphate sorption kinetics were measured on aggregates and on samples that had been disaggregated by sonication. For each aggregate type and initial P concentration, 0.5 g of aggregates was placed in each of six 30-ml glass-centrifuge tube. The aggregates were prewetted with drops of deionized water, and 10 ml of deionized water was added to each tube. Half of samples were disaggregated by

sonication for 1.5 min at 100 W. The procedure used to measure phosphate sorption kinetics was similar to that described for 48-h sorption experiments, except that the initial solution volume (25 ml) contained 0.02 μCi ml^{-1} ^{32}P-H$_3$PO$_4$ and total P concentrations of either 0.12 or 1.2 mM KH$_2$PO$_4$ in 0.015 M NaCl as background electrolyte. Aggregated and disaggregated samples were prepared in triplicate for each initial P concentration and three reaction temperatures. Initial suspension pH of each sample was adjusted to pH 5. The samples were shaken in a constant temperature chamber at 20, 30, and 40 °C on an end-over-end shaker at 90 cycles/min for 403 h (about 17 d). At each of nine sampling times, ranging from 8 min to 403 d, samples were centrifuged for 3 min at 1500 rpm, and a 0.2-ml aliquot was withdrawn from each tube. Each 0.2-ml aliquot was added to 5 ml of scintillation cocktail, and counted for 5 min on a Packard Tricarb 1500 liquid scintillation counter (Downer's Grove, IL).

Supernatant P concentrations were calculated with the equation:

$$Final\ conc\ of\ P = {}^{32}P_{final}/{}^{32}P_{blank} \times initial\ P\ conc \qquad (4.4)$$

Phosphate sorption kinetics are expressed as solution-phase $P_{final}/P_{initial}$ vs time, rather than as P sorbed vs time, because the fractional solution concentration gives more information about the extent of sorption at each time.

Results and Discussion

Phosphate Sorption and Desorption

Phosphate sorption isotherms for 48-h reaction show that there generally was no difference in P sorption between aggregated and disaggregated samples (Figure 4.1). The only exception was the A-horizon microaggregates of both soils at high P concentrations, where aggregated samples sorbed less P than did disaggregated samples. This trend was observed for both the Yellow-Red and the Dark-Red Latosol. Because these aggregates are relatively stable during P sorption and shaking (Chapter 3), sonication may be necessary to disrupt the aggregates and allow sorption sites from aggregate interiors to come into direct contact with the bulk solution. No such effect of disaggregation was observed for P sorption by B-horizon microaggregates, even though their stability during P sorption and shaking was also higher than large aggregates (Chapter 3). One possible explanation for the different effect of sonication on P sorption by A and B horizon microaggregates is that the B horizon microaggregates may be so stable that sonication does not effectively disaggregate them.

Aggregate size only affected P sorption for A-horizon aggregates, not B-horizon aggregates (Figure 4.1). For both soils, the large A-horizon aggregates sorbed more P than did the microaggregates, probably because the larger aggregates contained more DCB-extractable Fe and Al oxides and more goethite (Table 2.2). In the B horizon, aggregate size did not have a significant effect on P sorption (Figure 4.1).

For both soils and aggregate sizes, B-horizon aggregates sorbed about twice as much P as did A-horizon aggregates at all but the 0.12 mM initial P concentration. The greater P sorption by B than A horizons probably is due to the A-horizon's higher organic matter content (Table 2.2) and a resulting net negative
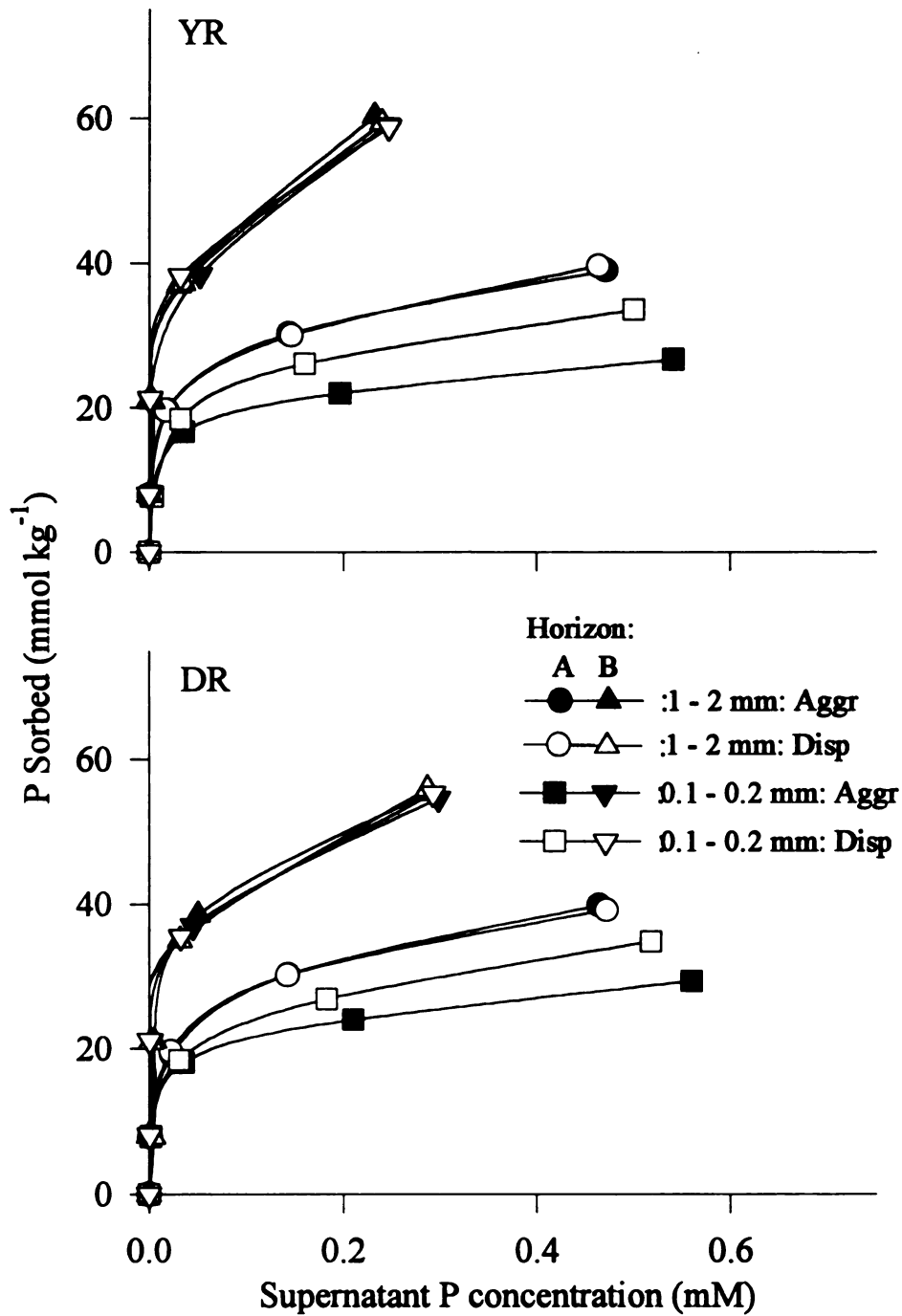
Figure 4.1. Phosphate sorption isotherms (20 °C, 48-h reaction) for two aggregate size fractions of A and B horizons of a Yellow-Red Latosol (top) and a Dark-Red Latosol (bottom), under disaggregated and aggregated conditions.

charge (Chapter 3). A recent study by Afif et al. (1995) showed that over the time period of years, phosphate can eventually displace organic matter from oxide sorption sites in A horizons, such that the true thermodynamic P sorption capacity of A horizons is comparable to that of B horizons. A "true" P sorption capacity of the B horizon samples cannot be determined from the present experiments because the sorption isotherms did not reach a plateau at the highest P concentration (Figure 4.1). Phosphate sorption by the Yellow-Red Latosol was similar to that of the Dark-Red Latosol (Figure 4.1). In B-horizon aggregates, the Yellow-Red Latosol, which has more goethite and a low Hm:Gt ratio (Table 2.2), sorbed more P than did the Dark-Red Latosol, which has less goethite. This result agrees with previous studies (Bigham et al., 1978; Curi and Franzmeier, 1984) wherein soils with more goethite (low Hm:Gt ratios) sorbed more phosphate that did soils with less goethite.

The effect of temperature on Langmuir b values, which ideally represent sorption maxima, is shown in Table 4.1. The Langmuir equation is not strictly applicable to these isotherms, especially for the B horizons, because none had reached a true plateau as can be inferred from (Figure 4.1). The qualitative agreement between the data in Table 4.1 and Figure 4.1 show that this approach can provide useful results, even though the b values for the B horizon are not true sorption maxima. The Langmuir b values allow rapid comparison of the sorption data in tabular form.

The amount of desorbed P was also fit with the Langmuir equation to give a very rough estimate of the maximum desorbable P over the concentration range used in this study. Desorbable P concentrations are relevant for soil fertility because they represent the most readily bioavailable sorbed P. However, the "desorbable maximum" (Langmuir b values for desorbed P) give no information

Table 4.1. Effect of temperature and dispersion on Langmuir equation b values for 48-h P sorption and 24 h desorption in different aggregate sizes of A and B horizons of two Oxisols.

Horizon	Aggr Size	Dispersion	Sorption[1]		Desorbable[2]	
			20 °C	40 °C	20 °C	40 °C
				mmol kg^{-1}		
Yellow-Red Latosol						
A	1 - 2 mm	Aggr	39.4	49.0	9.1	10.7
		Disp	40.1	49.5	9.1	9.2
	0.1 - 0.2 mm	Aggr	26.8	42.7	7.9	8.1
		Disp	34.2	40.0	10.6	9.0
B	1 - 2 mm	Aggr	61.6	66.9	8.4	8.5
		Disp	60.0	65.2	7.3	7.2
	0.1 - 0.2 mm	Aggr	60.1	64.0	7.3	6.3
		Disp	59.5	63.6	7.4	6.2
Dark-Red Latosol						
A	1 - 2 mm	Aggr	40.5	50.0	10.6	9.4
		Disp	39.7	49.7	9.6	9.1
	0.1 - 0.2 mm	Aggr	29.6	42.7	9.4	10.5
		Disp	35.2	44.2	8.8	9.2
B	1 - 2 mm	Aggr	56.4	61.8	9.3	7.0
		Disp	58.2	62.0	8.2	7.6
	0.1 - 0.2 mm	Aggr	55.4	60.8	8.4	7.1
		Disp	56.1	61.9	8.3	8.1
LSD	$\alpha = 0.05$		5.7	2.6	1.2	0.9
	$\alpha = 0.01$		8.0	3.7	1.7	1.4

1 - Values obtained from the linear form of Langmuir plot, equation 4.3.

2 - Values obtained from the linear form of Langmuir equation, using the amount of desorbed, instead of sorbed P in equation 4.3.

about the relationship between sorbed P concentration and desorbed P. In any case, they are useful for looking at the effect of temperature on P desorption.

Increasing temperature increased the maximum P sorbed, as can be seen in Table 4.1. The effect of temperature was higher in the A horizon aggregates. In this case, the effect of organic matter on delaying P sorption (Afif et al., 1995) is a possible explanation for the higher effect of temperature on A horizon material, since it could increase ligand exchange, and, eventually, A and B horizon aggregates can sorb similar amounts of P, since they have the same mineralogy (Table 1.1). The amount desorbed was similar at both 20 and 40 °C, despite the higher sorption at 40 °C. This suggest that higher temperature caused P ions to diffuse to less accessible sites and/or some P complexes changed from monodentate to bidentate that is much more difficult to desorb (Kafkafi, 1967; Hingston, 1974).

Kinetics of P sorption

The initial reaction rate (from zero to 8 min) is higher for dispersed than it is for aggregated material, mainly in the B horizon aggregates, as can be seen by the lower final/initial ratio in Figures 4.2 and 4.3. Liquid-phase diffusion, from the bulk solution to the interior of aggregates, seems to be limiting P sorption, as suggested by Skopp (1986), whereas more sites became immediately available when aggregates were initially dispersed by sonication. The ratio of final/initial P sorption at 8 min in the dispersed aggregates was much lower at low initial P concentration, mainly in the B horizon material. The effect of temperature was similar for all samples. High temperature (40 °C) caused the final/initial P ratio at 8 minutes to decrease, and thus increased P sorption. The YR soil (Figure 4.2) sorbed more P at 8 min than did the DR soil (Figure 4.3) in aggregated material, mainly at higher initial P concentration. This shows the higher reactivity of aggregates with lower Hm/Gt ratio, more goethite.
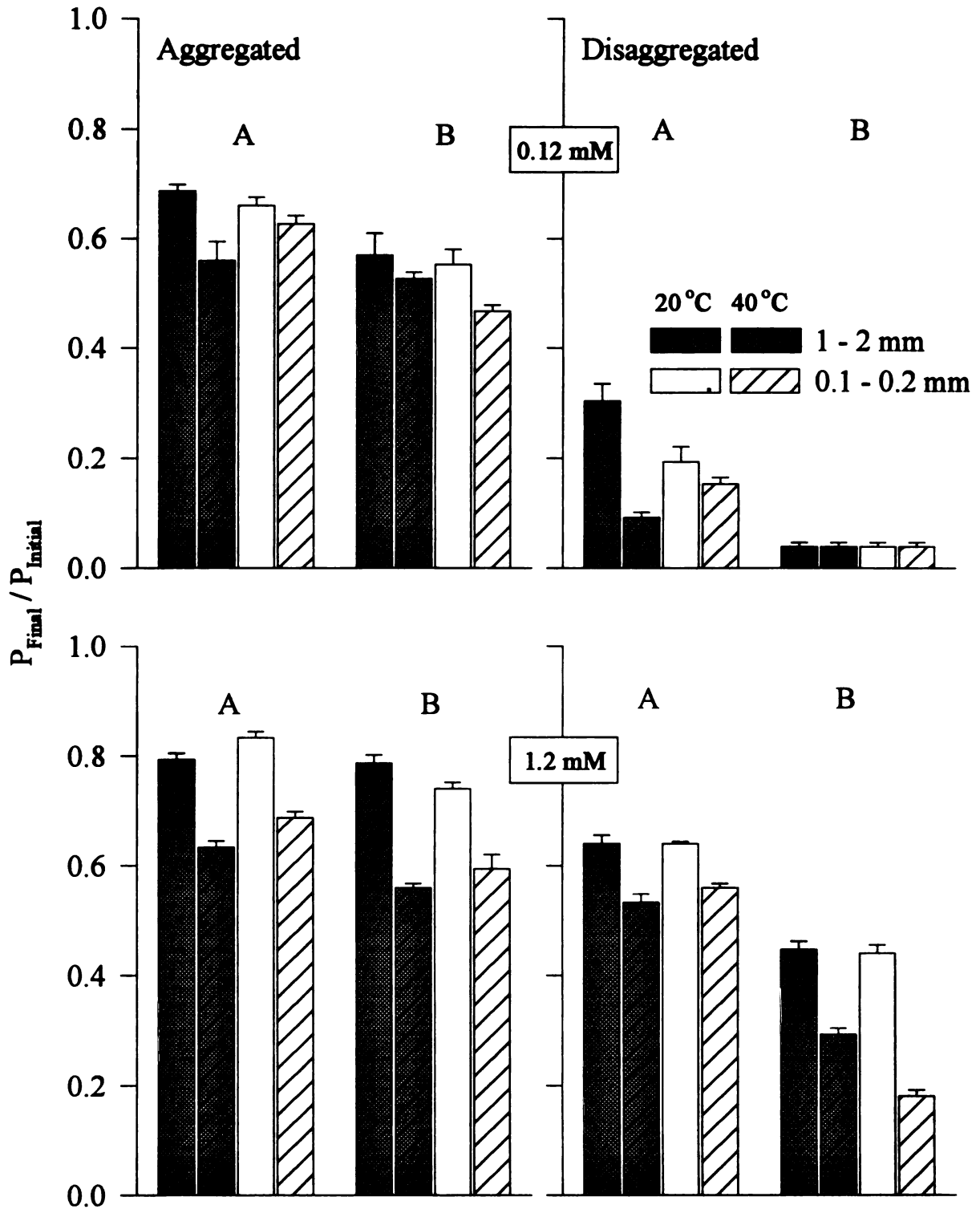
Figure 4.2. Effect of temperature and dispersion on solution-phase final/initial P concentrations after 8-min reaction for two aggregate sizes of A and B horizons of a Yellow-Red Latosol at two initial P concentrations.
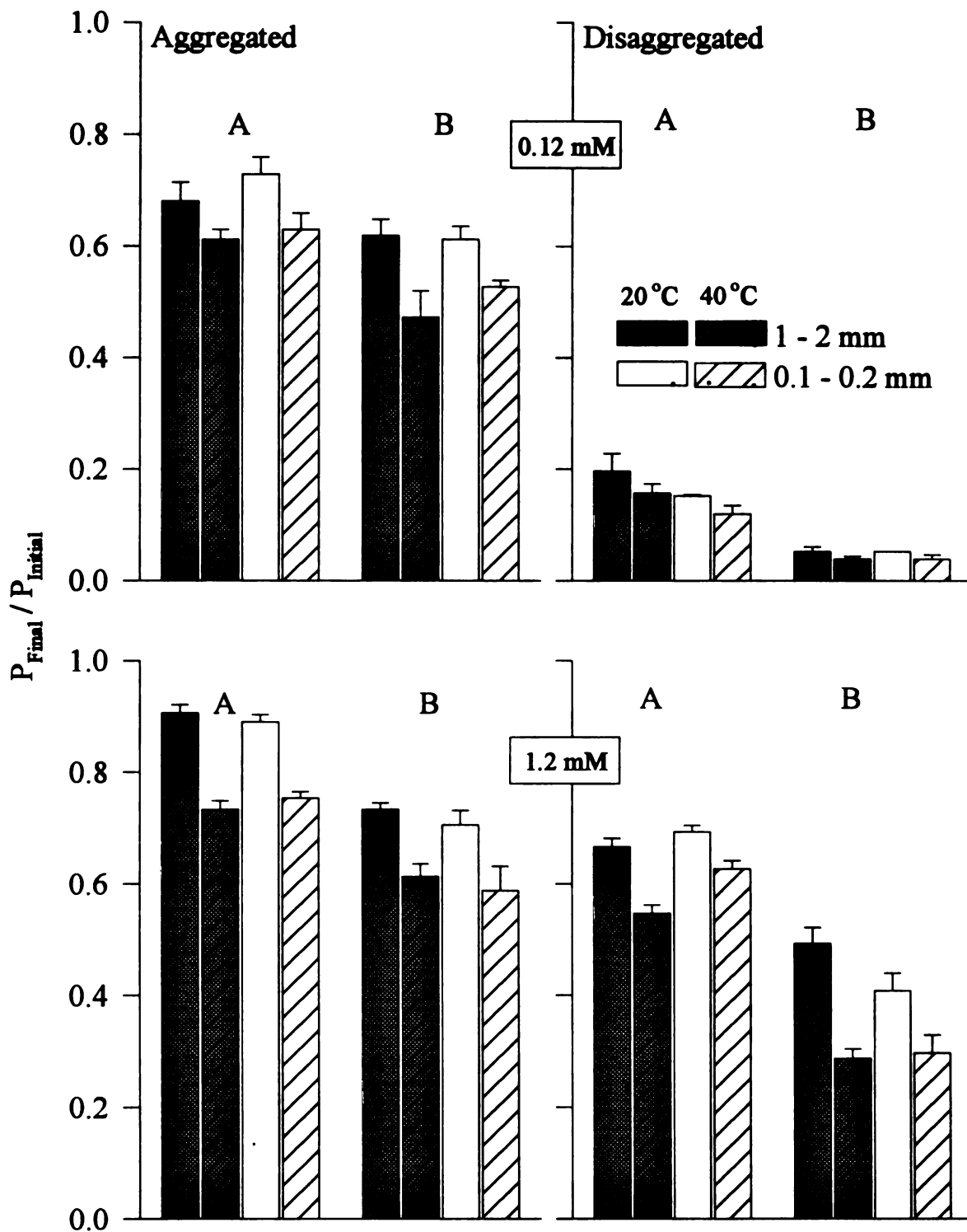
Figure 4.3. Effect of temperature and dispersion on solution-phase final/initial
P concentrations after 8-min reaction for two aggregate sizes of A and B horizons
of a Dark-Red Latosol at two initial P concentrations.

The curves in Figures 4.4 to 4.7 show that the main difference on P sorption between the two aggregate sizes, or between dispersed and aggregated material, occurs at early times. There is no difference at 1200 min (20 h) at low initial P concentration (Figures 4.4 and 4.6). The difference between aggregated and dispersed material decreases with time. This suggest that liquid- and solid-phase diffusion of phosphate has overcome the effect of aggregation on phosphate sorption kinetics at times longer than 20 h. An additional explanation is that dispersion of aggregates, caused by P sorption and shaking, exposes new surface sites, increasing P sorption. Therefore, the effect of aggregates at longer times will depend on how stable are the aggregates and how pH-dependent charged is the soil material, for aggregation to be affected by P sorption. The higher the effect of P on clay dispersion, the smaller the influence of aggregation on the rate of reactions, at longer times. However, aggregates have great effect on P sorption kinetics since most of P is sorbed at short time.
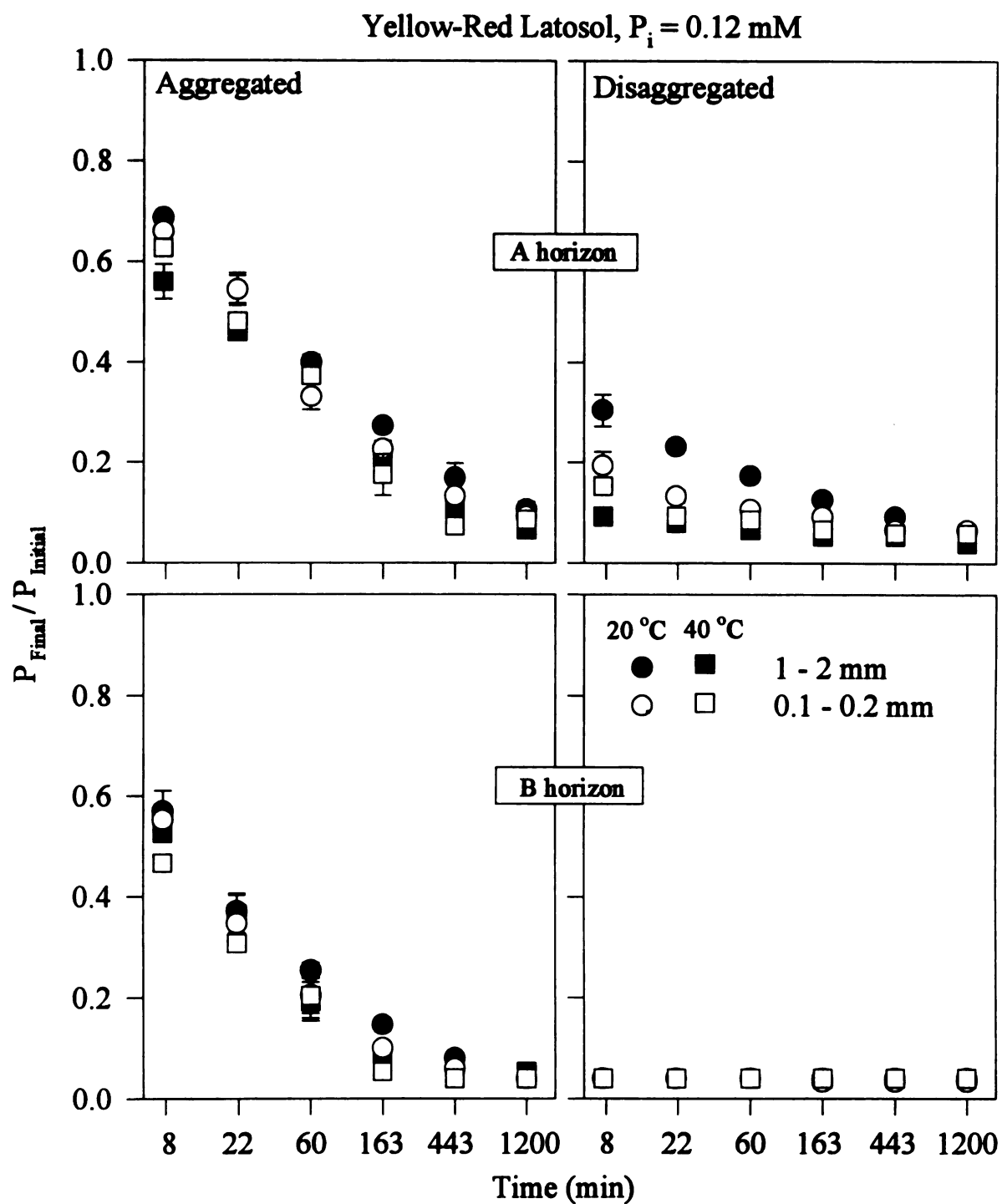
Figure 4.4. Effect of aggregate size and temperature on P sorption kinetics, semilog scale, for A and B horizons of a Yellow-Red Latosol under aggregated and disaggregated conditions.(Initial P concentration = 0.12 mM)
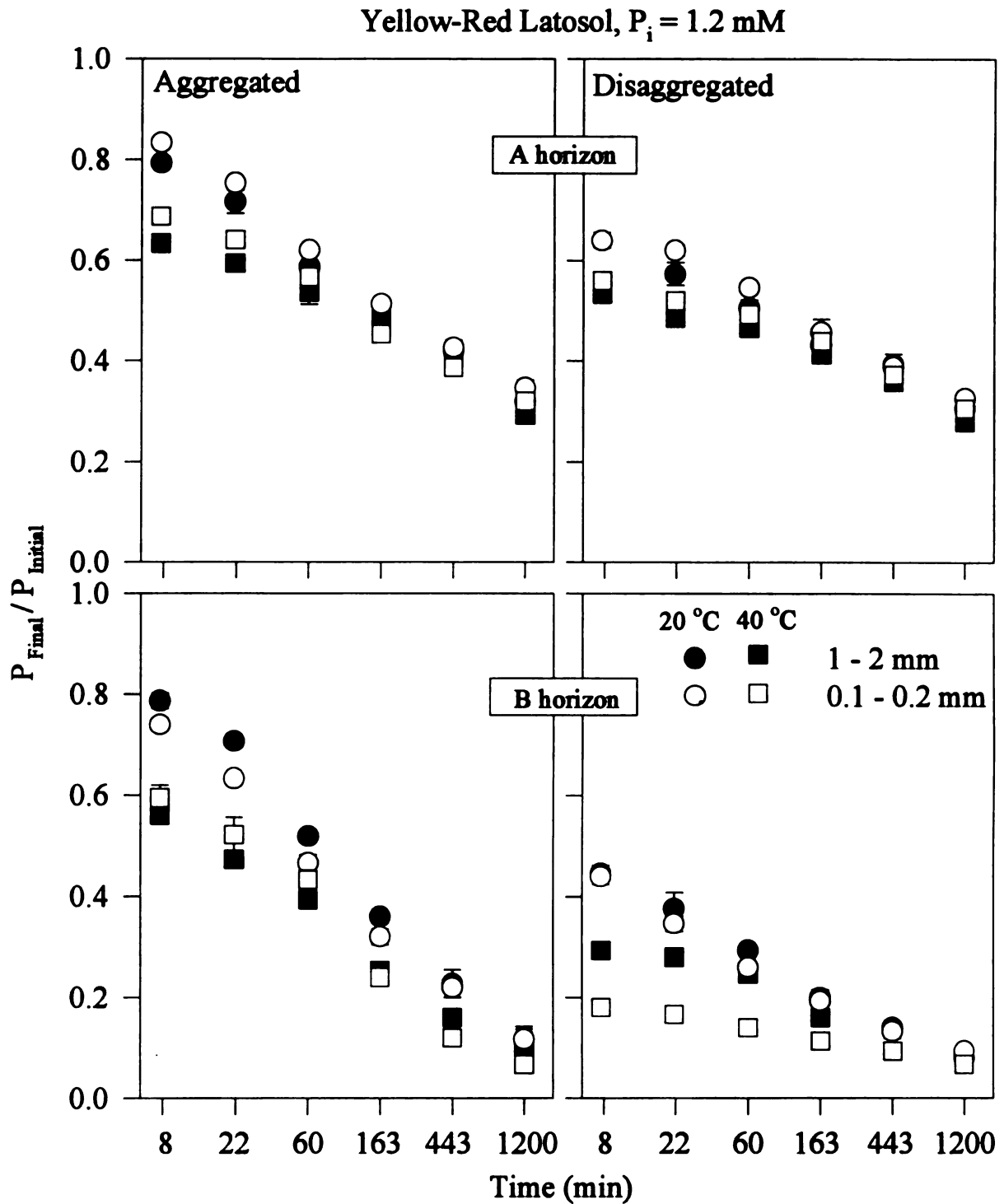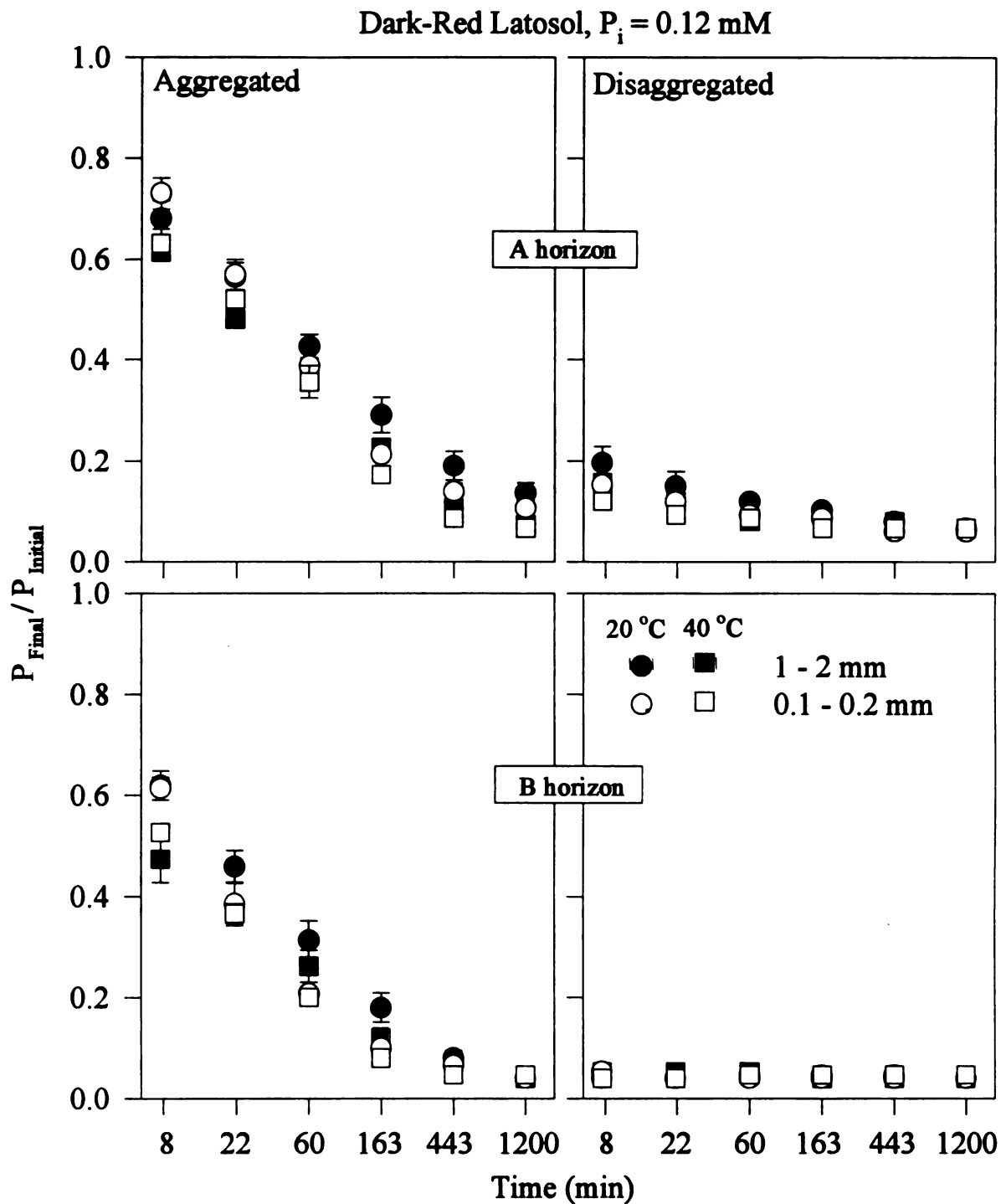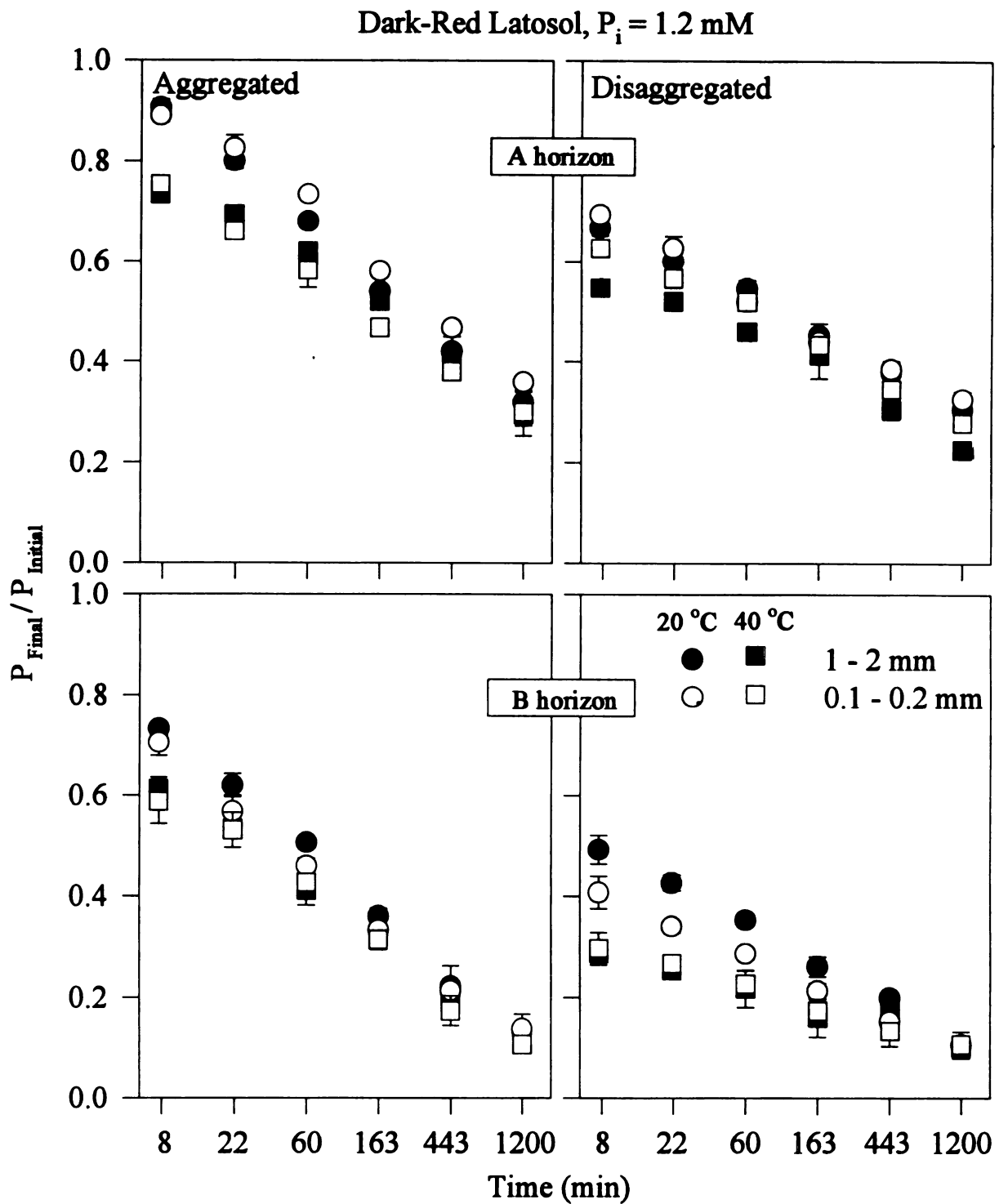
Figure 4.5. Effect of aggregate size and temperature on P sorption kinetics, semilog scale, for A and B horizons of a Yellow-Red Latosol under aggregated and disaggregated conditions.(Initial P concentration = 1.2 mM)

Figure 4.6. Effect of aggregate size and temperature on P sorption kinetics, semilog scale, for A and B horizons of a Dark-Red Latosol under aggregated and disaggregated conditions.(Initial P concentration = 0.12 mM)

Figure 4.7. Effect of aggregate size and temperature on P sorption kinetics, semilog scale, for A and B horizons of a Dark-Red Latosol under aggregated and disaggregated conditions.(Initial P concentration = 1.2 mM)

Conclusions

Aggregate size only affected phosphate sorption for A-horizon aggregates. The higher DCB-extractable Fe and Al oxides and more goethite are the most probable factors causing P sorption to be higher on the small aggregates of A horizons. For both soils and aggregate sizes, B-horizon aggregates sorbed about twice as much as did A-horizon aggregates.

Disaggregation of the soil material prior the sorption kinetics measurements increased the rate of P sorption, which shows that liquid-phase diffusion is rate limiting P sorption. The effect of aggregation was higher at early times. This shows that the fast step of the P sorption kinetics is more likely to be affected by soil aggregation.

Bibliography

Afif, E., V. Barron, and J. Torrent. 1995. Organic matter delays but not prevent phosphate sorption by cerrado soils from Brazil. Soil Sci. 159:207-211.

Arca, M.N., and S.B. Weed. 1966. Soil aggregation and porosity in relation to contents of free iron oxide and clay. Soil Sci. 101:164-170.

Barberis, E., F.A. Marsan, V. Boero, and E. Arduino. 1991. Aggregation of soil particles by iron oxides in various size fractions of soil horizons. J. Soil Sci. 42:535-542.

Bigham, J.M., D.C. Golden, S.W. Buol, S.B. Weed, and L.H. Bowen. 1978. Iron oxide mineralogy of well-drained Ultisols and Oxisols: II. Influence on color, surface area, and phosphate retention. Soil Sci. Soc. Am. J. 42:825-830.

Bolan, N.S., N.J. Barrow, and A.M. Posner. 1985. Describing the effect of time on sorption of phosphate by iron and aluminum hydroxides. J. Soil Sci. 36:187-197.

Chesters, G., O.J. Attoe, and O.N. Allen. 1957. Soil aggregation in relation to various soil constituents. Soil Sci. Soc. Am. Proc. 21:272-277.

Curi, N., and D.P. Franzmeier. 1984. Toposequence of Oxisols from the Central Plateau of Brazil. Soil Sci. Soc. Am. J. 48:341-346.

Giovanini, G., and P. Sequi. 1976. Iron and aluminum as cementing substances of soil aggregates. II Changes in stability of soil aggregates following extraction of iron and aluminum by acetylacetone in a non-polar solvent. J. Soil Sci. 27:148-153.

Goldberg, S. 1989. Interaction of aluminum and iron oxides and clay minerals and their effect on soil physical properties: a review. Commun. Soil Sci. Plant Anal. 20:1181-1207.

Hingston, F.J., A.M. Posner, and J.P. Quirk. 1974. Anion adsorption by goethite and gibbsite. II: Desorption of anions from hydrous oxide surfaces. J. Soil Sci. 25:16-26.

Kafkafi, U., A.M. Posner, and J.P. Quirk. 1967. Desorption of phosphate from kaolinite. Soil Sci. Soc. Amer. Proc. 31:348-353.

Madrid, L., and P. De Arambarri. 1985. Adsorption of phosphate by iron oxides in relation to their porosity. J. Soil Sci. 36:523-530.

Murphy, J., and J.P. Riley. 1962. A modified single solution method for determination of phosphate in natural waters. Analitica Chemica Acta. 27:31-36.

Parfitt, R.L. 1978. Anion adsorption by soils and soil materials. Advances in Agronomy. 30:1-50.

Parfitt, R.L. 1989. Phosphate reactions with natural allophane, ferrihydrite and goethite. J. Soil. Sci. 40:359-369.

Sanyal, S.K., S.K. De Datta, and P.Y Chan. 1993. Phosphate sorption-desorption behavior of some acidic soils of South and Southeast Asia. Soil Sci. Soc. Am. J. 57:937-945.

Skopp, J. 1986. Analysis of time-dependent chemical processes in soils. J. Environ. Qual. 15:205-213.

Sollins, P. 1991. Effects of soil microstructure on phosphorus sorption in soils of the Humid Tropics. In: H. Tiessen, D. Lopez-Hernandez, and I.H. Salcedo. (ed) Phosphorus cycles in terrestrial and aquatic ecosystems. Regional Workshop 3: South and Central America. Maracay, Venezuela. November/December 1989.

Willett, I.R., C.J. Chartres, and T.T. Nguyen. 1988. Migration of phosphate into aggregated particles of ferrihydrite. J. Soil Sci. 39:275-282.

General Conclusions

The results of this research show that aggregates can differ in composition even at the < 2-mm fraction of the soil. Differences in composition may have caused in differences in aggregate stability and affected extraction of Fe and Al by dithionite-citrate-bicarbonate and ammonium oxalate. Disaggregation increased the amount of Fe and Al extracted by DCB. Thus, the amount of Fe and Al extracted from aggregated material with a single extraction is not the true amount of those oxides in samples. More than four extractions are necessary for the true amount of Fe and Al to be extracted by DCB from aggregated material.

Phosphate sorption had no effect on clay dispersion in A horizon aggregates. In B horizon aggregates, phosphate sorption initially caused a decrease in flocculation by decreasing the amount of positive charge. As additional P sorption caused the soil material to became negatively charged, phosphate sorption increased the amount of clay dispersion by increasing particle repulsion. However, when phosphate sorption was at least 35 mmol kg^{-1}, additional P sorption did not cause additional clay dispersion in the B horizon material. At this level of sorbed P, about 80 % of the clay in large aggregates and 40 % in small aggregated was dispersed. The amounts of P sorption that would occur in response to fertilization may greatly increase the erodibility of the B horizon.

Phosphate sorption rate was affected by aggregation. The fast P sorption reaction, which occurs at short times, is more likely to be affected by aggregation. The difference of P sorption kinetics between aggregated and disaggregated material decreases as time increases up to about 1200 min (20 h). After this time, both aggregated and disaggregated material have similar sorption rate.
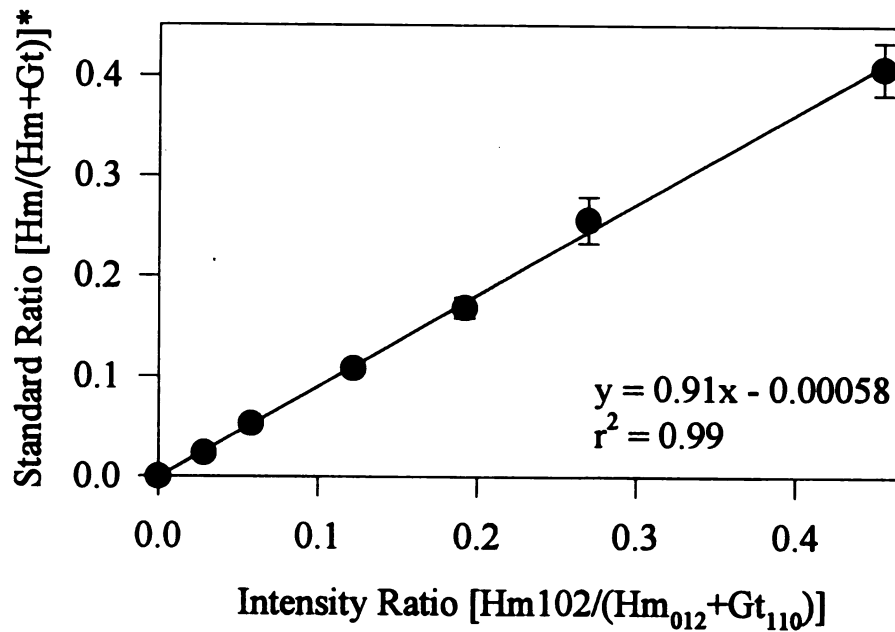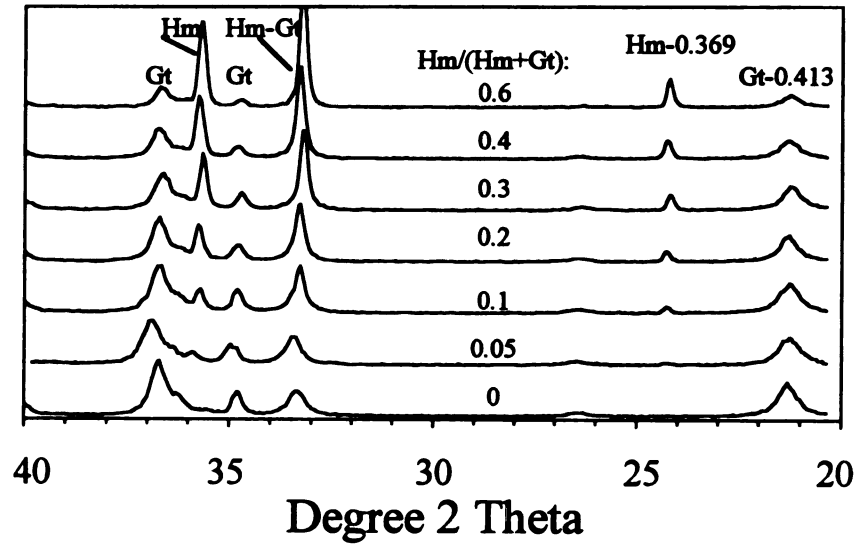
APPENDICES

Appendix A1

Effect of time of sonication in 1 mM NaOH on clay dispersed/total clay in a Yellow-Red (YR) and a Dark-Red Latosol (DR).
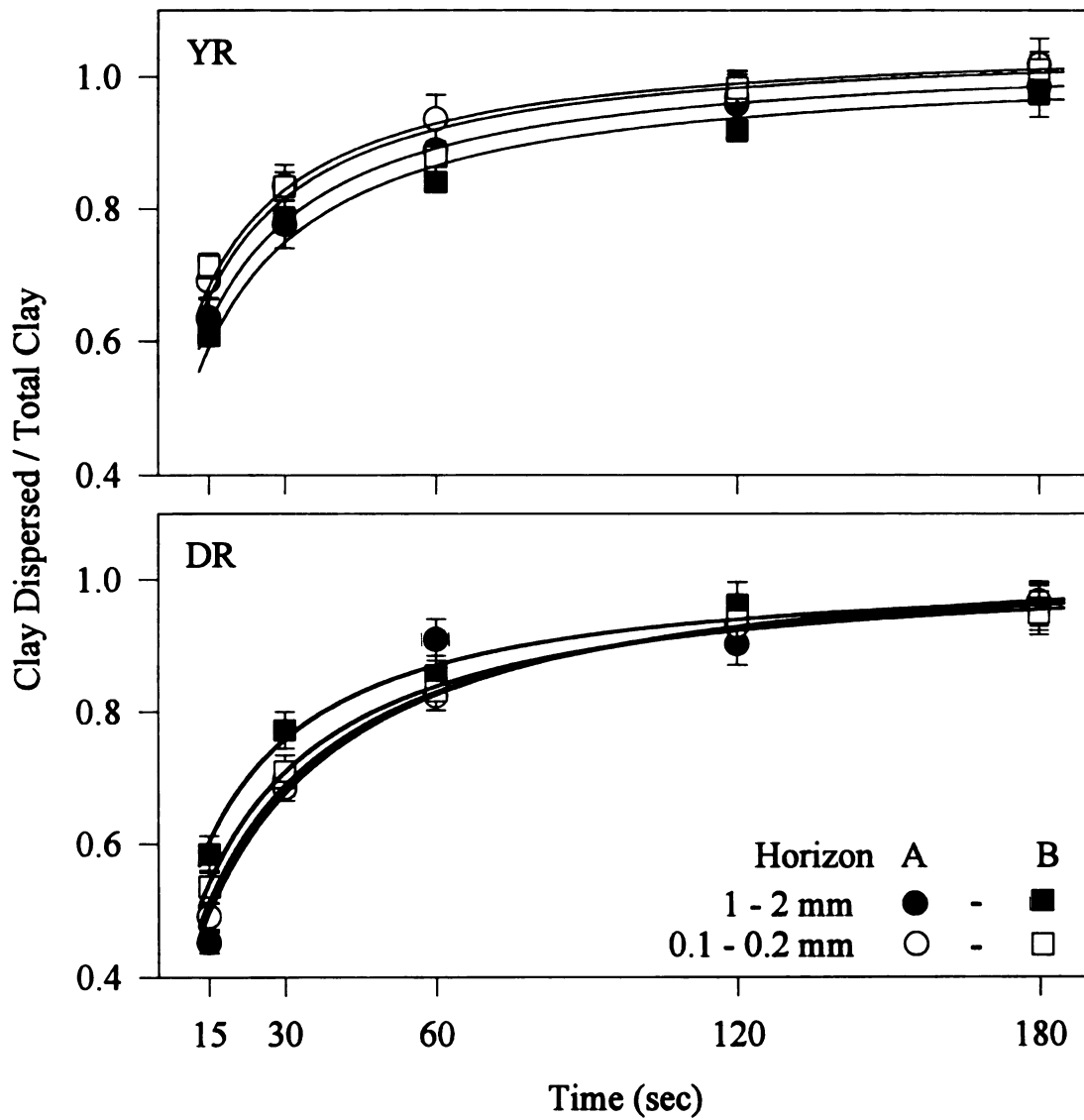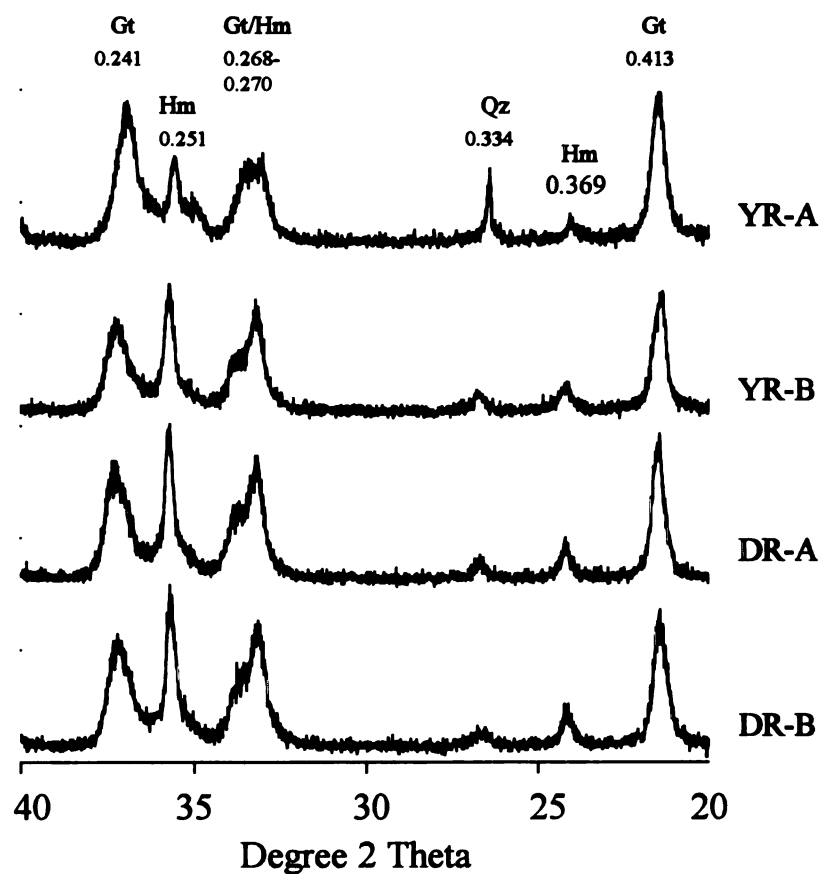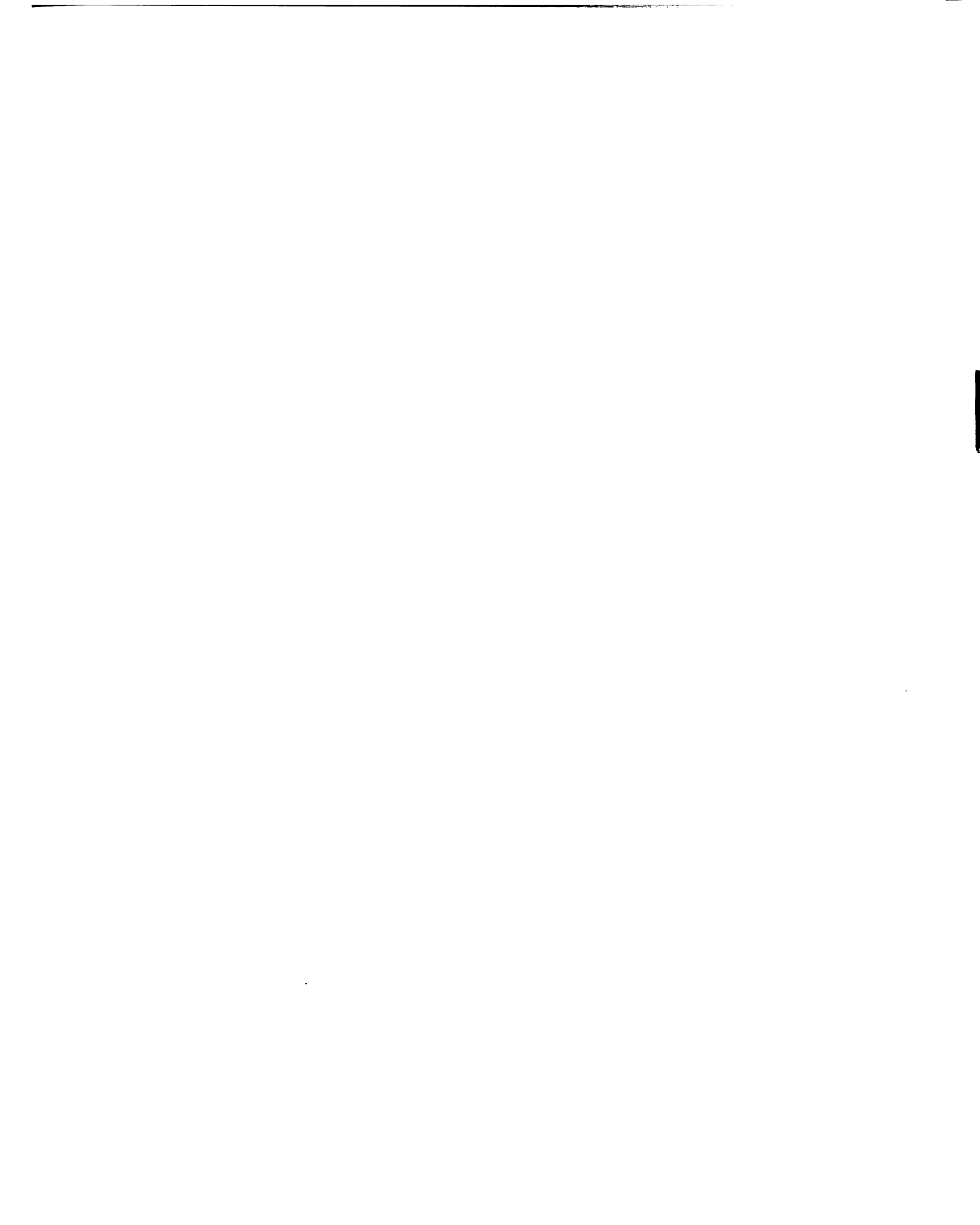
Appendix A2

X-ray diffraction patterns of standards (* normalized for Fe content in Hm and Gt), and standard curve of the hematite/goethite ratio, used to calculate the proportions of hematite and goethite in the aggregate samples.

Appendix A3

X-ray diffraction patterns of the clay fraction of A and B
horizons of a Yellow-Red and a Dark-Red Latosol, treated with
5M NaOH to concentrate iron oxides. Gt: goethite; Hm: hematite;
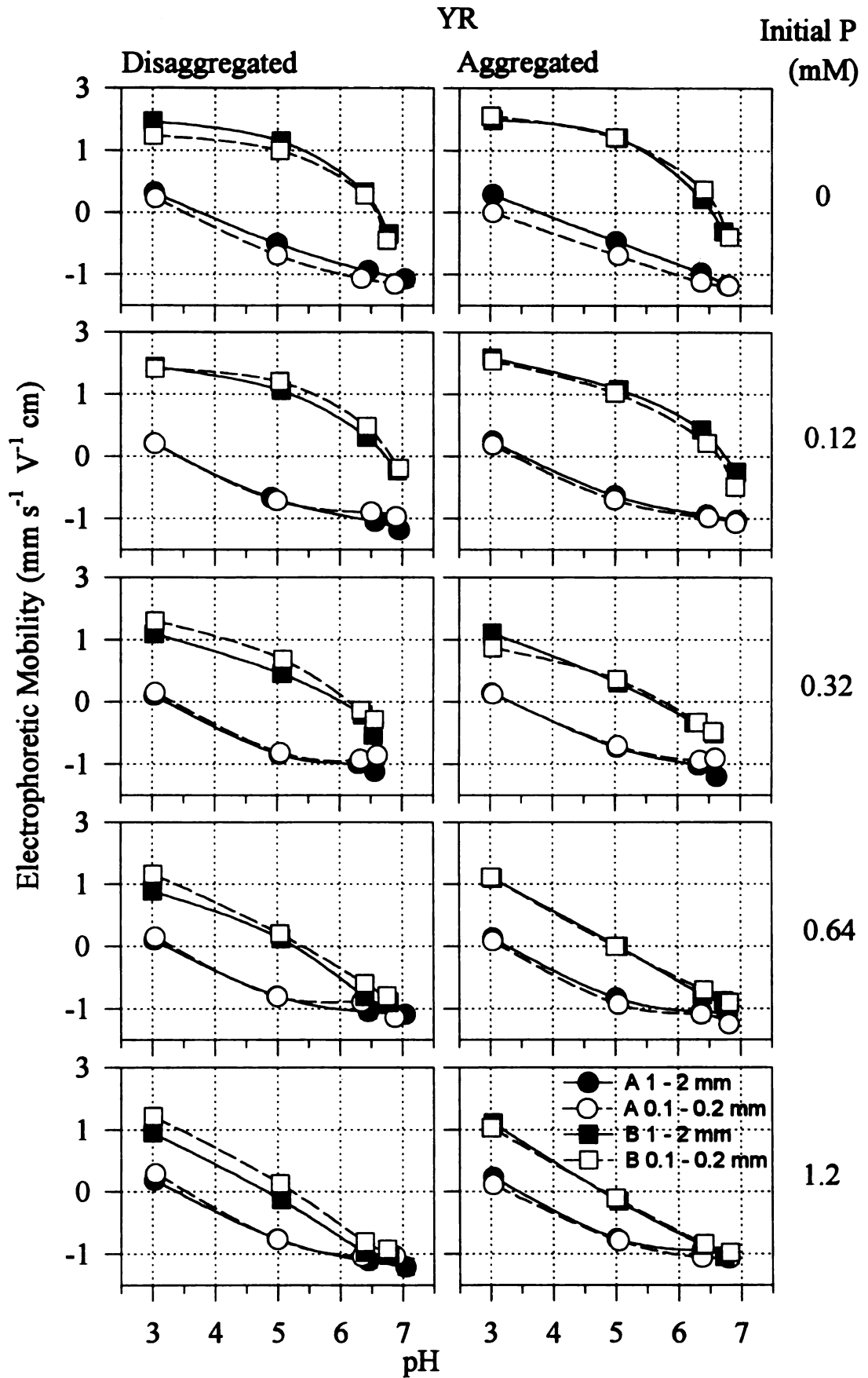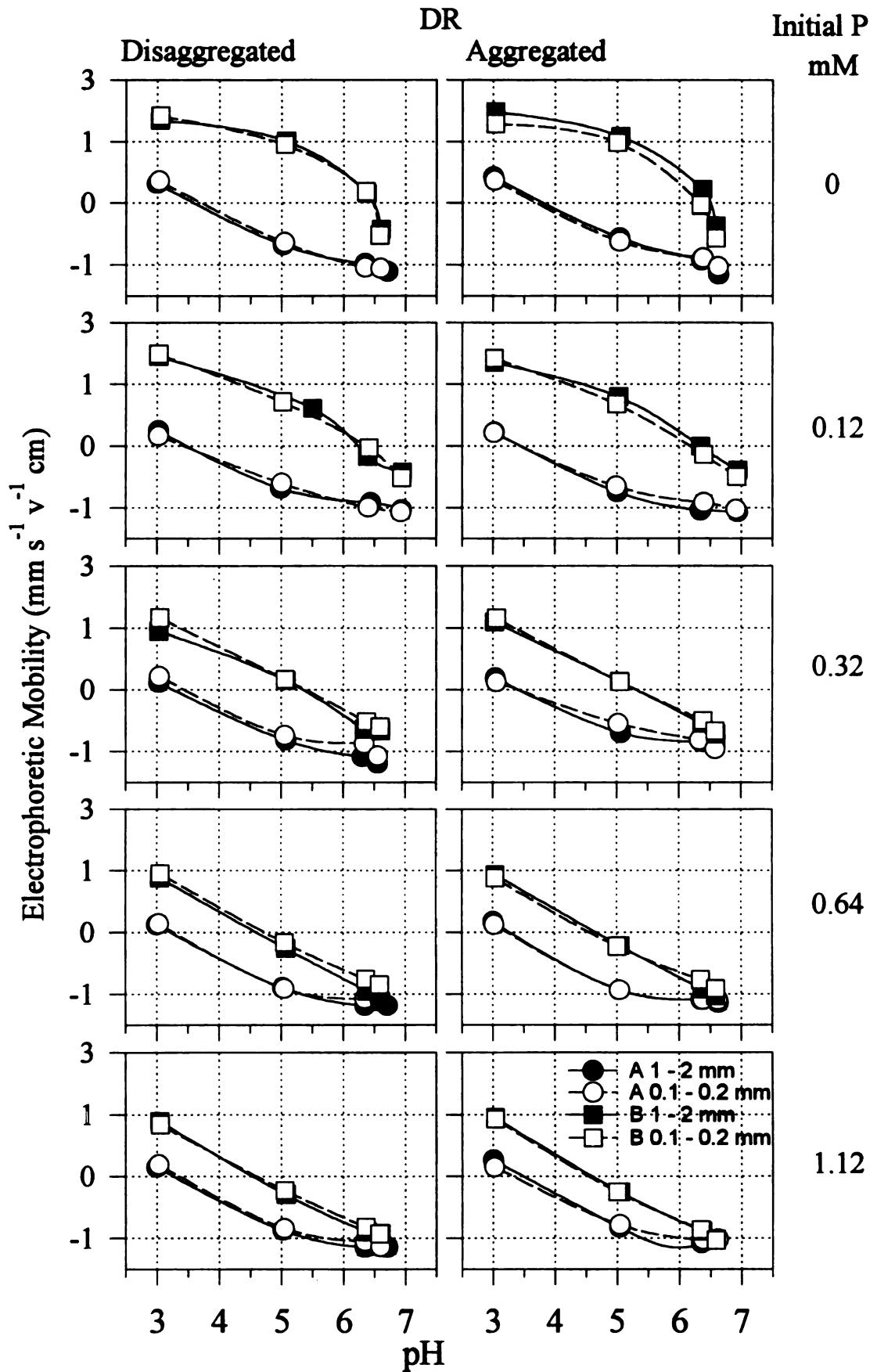Qz: quartz. Numbers represent d spacing (nm).

Appendix B1

Effect of pH, aggregate size, and initial P concentration on electrophoretic mobility of A and B horizons of a Yellow-Red Latosol (Appendix B1-1, YR) and a Dark-Red Latosol (Appendix B1-2, DR).
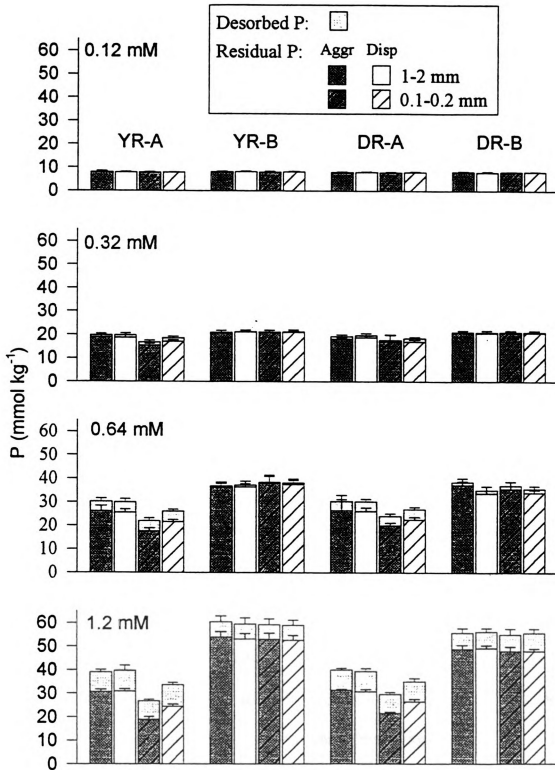
Appendix B1-1

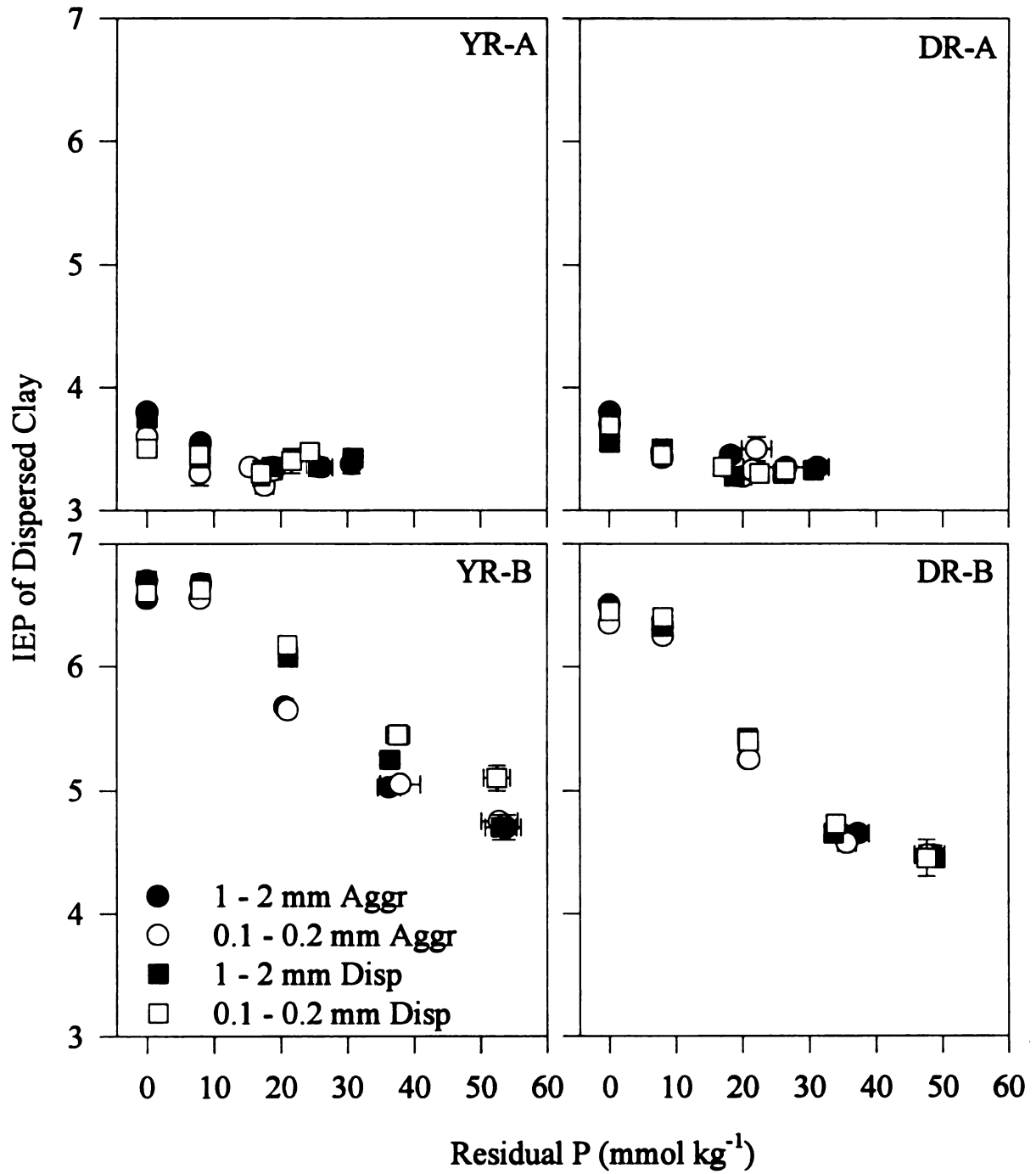**Appendix B1-2**

Appendix B2

Effect of aggregate size on residual sorbed P (bottom bars), desorbed P (upper bars), and total sorbed (combined bars height) at four initial P concentrations for A and B horizons of Yellow-Red (YR) and Dark-Red (DR) Latosols.
(under aggregated and disaggregated initial conditions)
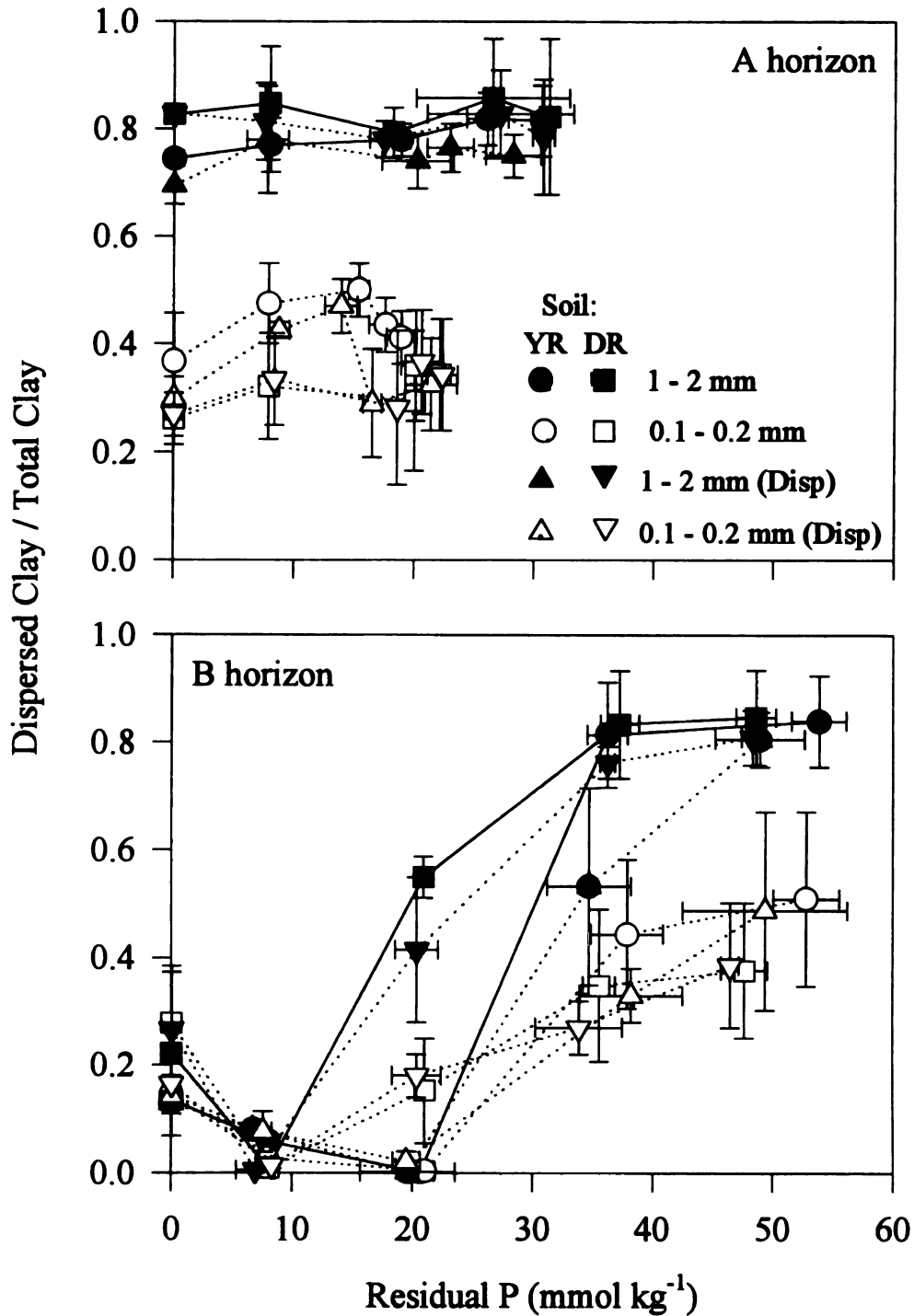
Appendix B2

Appendix B3

Effect of residual P and aggregate size on isoelectric points of dispersed clay from A and B horizons of Yellow-Red (YR) and Dark-Red (DR) Latosols under aggregated and dispersed initial conditions.
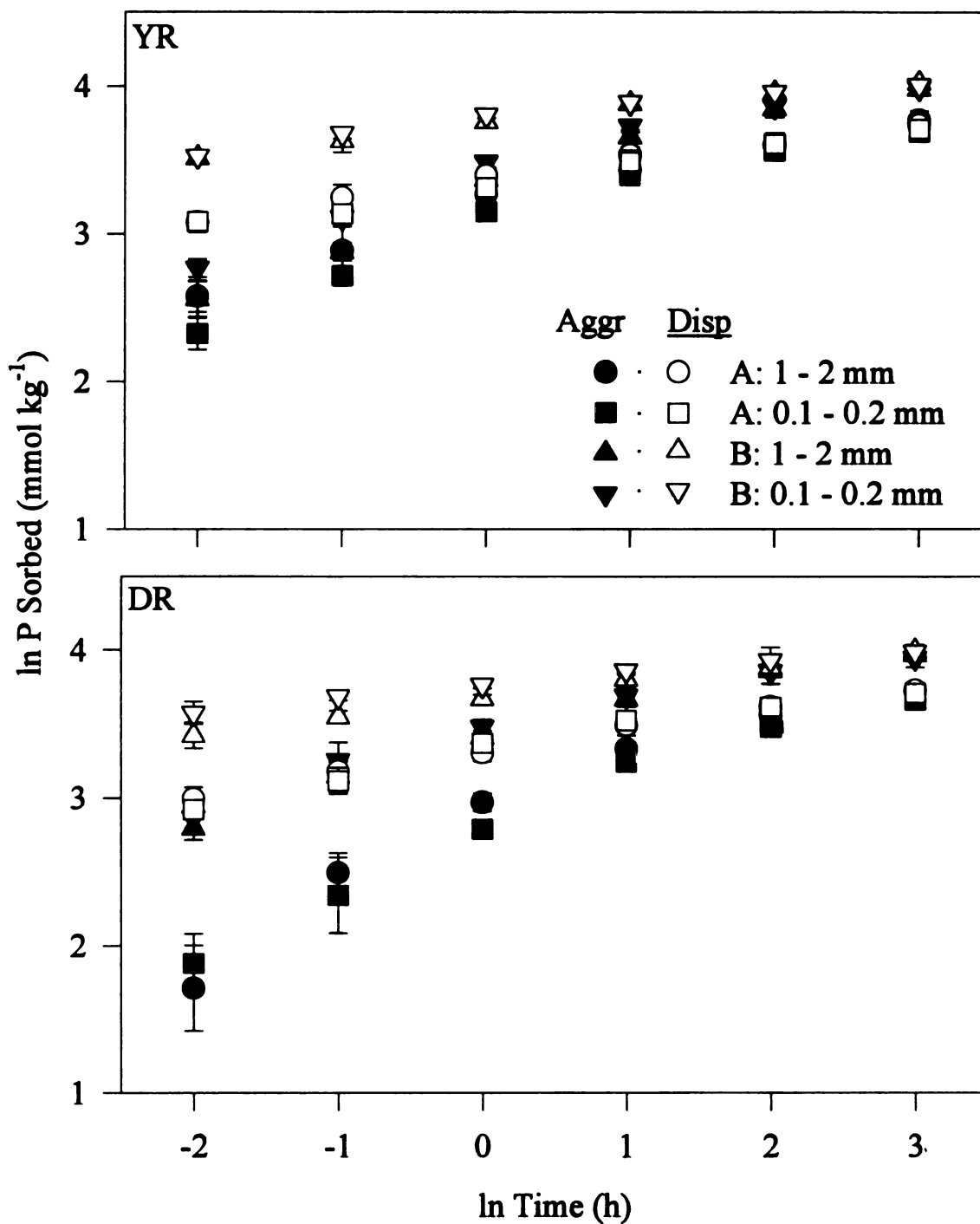
Appendix B4

Effect of residual sorbed P and aggregate size on dispersed/total
clay for A and B horizons of Yellow-Red Latosol (YR) and Dark-
Red Latosol (DR) under aggregated and dispersed initial conditions.

Appendix C1

Phosphate sorption as a function of time, ln plot, of two aggregate size fractions of A and B horizons of a Yellow-Red and a Dark-Red Latosol, under aggregated and disaggregated initial conditions, 1.2 mM initial P concentration, at 20 °C.
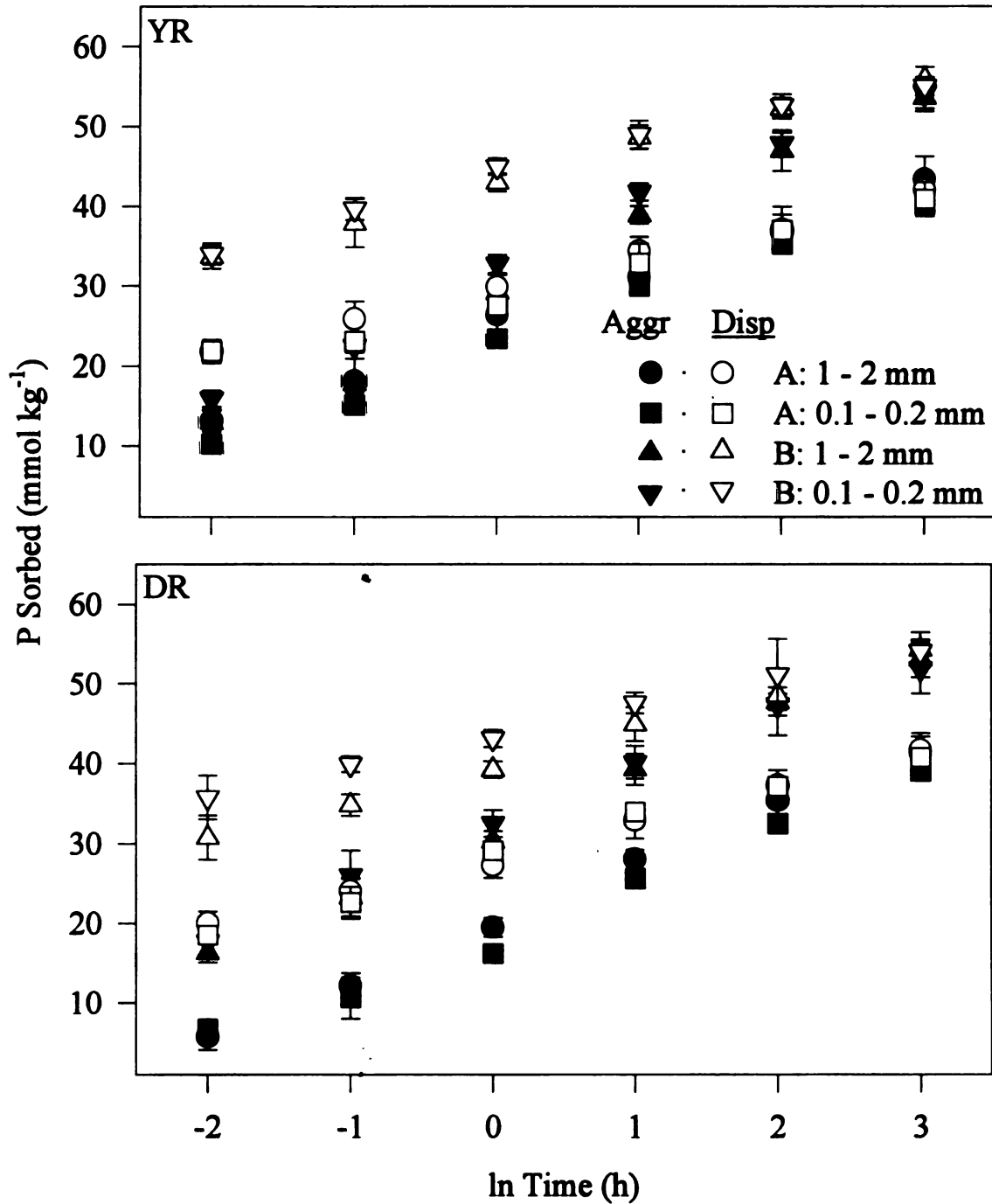
Appendix C2

Rate constant and activation energy of P sorption on two aggregate size fractions of A and B horizons of a Yellow-Red Latosol and a Dark-Red Latosol.

Horizon	Aggr	Aggregated		Disaggregated	
		k	Ea	k	Ea
		h^{-1}	kJ mol^{-1}	h^{-1}	kJ mol^{-1}
		Yellow-Red Larosol			
A	1 - 2	0.35	4.99	0.46	2.89
		(0.04)	(1.58)	(0.04)	(1.54)
	0.1 - 0.2	0.33	4.92	0.45	2.54
		(0.02)	(0.46)	(0.03)	(1.06)
B	1 - 2	0.41	7.34	0.61	1.97
		(0.05)	(1.71)	(0.16)	(0.22)
	0.1 - 0.2	0.46	4.69	0.62	3.02
		(0.06)	(1.95)	(0.18)	(0.23)
		Dark-Red Latosol			
A	1 - 2	0.26	7.2	0.44	3.76
		(0.04)	(3.17)	(0.04)	(1.28)
	0.1 - 0.2	0.24	9.46	0.44	2.01
		(0.04)	(1.98)	(0.03)	(0.85)
B	1 - 2	0.45	4.14	0.62	4.15
		(0.06)	(1.83)	(0.05)	(1.59)
	0.1 - 0.2	0.49	3.05	0.70	1.93
		(0.06)	(1.37)	(0.05)	(0.70)

Numbers in parenthesis are the standard deviation of triplicate samples.

Appendix C3

Phosphate sorption as a function of time, semilog plot, of two aggregate size fractions of A and B horizons of a Yellow-Red and a Dark-Red Latosol under aggregated and disaggregated initial conditions, 1.2 mM initial P concentration, at 20 °C.